Nonlinear propagation of terahertz pulses in ammonia vapor

O. M. Fedotova,[1] O. K. Khasanov,[1,*] G. A. Rusetsky,[1] J. Degert,[2] and E. Freysz[2]

[1]*Scientific-Practical Material Research Centre, Belarus National Academy of Sciences, 19 Brovki Street, Minsk 220072, Belarus*

[2]*Laboratoire Ondes et Matiè re d'Aquitaine, UMR 5798, Université Bordeaux 351 Cours de la Libération, 33405 Talence, France*

(Received 21 September 2014; published 24 November 2014)

We consider the propagation of terahertz (THz) pulses resonant with the lowest rotational levels in ammonia vapors at room temperature. We demonstrate a quasisimultonic regime of propagation for two-color THz pulses (their lossless simultaneous propagation with equal group velocities and stable envelopes at finite distances, like coupled solitons). The quasisimultons are formed by two pulses synchronized in time, the first one being intense and two humped with an area multiple of 4π, while the another one is weaker, one humped, and with an area much less than π. Two- and one-humped pulses have equal width and copropagate in ammonia vapor at the same group velocity. Moreover, the larger the dip of the two-hump pulse is, the weaker may be the one-humped pulse. The stability of this coupled state is provided by the fact that the two-humped pulse makes the medium transparent for the one-humped pulse. In its turn, the latter prevents the breakup of the former into separate pulses. It is established as well that a multihumped pulse with an odd or even number of humps and a hyperbolic secant pulse can behave like a simulton. In this case, the area of multihumped pulse equals to $2n\pi$, where n is the number of humps in the powerful pulse structure.

DOI: 10.1103/PhysRevA.90.053843 PACS number(s): 42.65.Tg, 42.65.Jx, 41.20.Jb

I. INTRODUCTION

Revolutionary changes in nonlinear physics often are related to the introduction of the concepts of soliton and strange attractor. Since then a number of processes occurring in nature have become clear and predictable. The history of solitons has always been associated with real applications. Soliton solutions arise, for example, in hydrodynamics, solid-state physics, biophysics, and nonlinear optics. Recently, many new kinds of optical solitons have been revealed. Besides temporal and spatial solitons, which have already become classical, by now, optical bullets, Bragg and gap solitons, discrete and vortex solitons, parametric and incoherent solitons, self-induced transparency (SIT) solitons (SIT-solitons), etc., have been investigated. A soliton (solitary wave) is a particlelike solution of a nonlinear differential equation, describing the excitation of finite energy having distinctive features. As a rule, a soliton retains both its shape and its velocity during propagation and under collision with other solitary waves. However, there are many examples when solitons do not retain their shape while propagating, moving at an accelerated speed, decomposing, or forming coupled states [1]. The soliton theory is connected with the theory of completely integrable nonlinear evolution equations, and soliton solutions may be defined using the inverse scattering transform method. Nevertheless, the value of numerical experiments in soliton research is indisputable. In reality, the governing equations are typically nonintegrable and therefore numerical methods may be especially effective for soliton studying in nonintegrable systems.

Soliton formation is a result of competitive process balance, i.e., dispersion and nonlinearity or diffraction and nonlinearity [2]. As for SIT solitons, they are observed in resonant two-level media when the width of an ultrashort pulse (USP) is short compared to dissipative relaxation times. In this case, the light-medium interaction represents stimulated absorption and emission of electromagnetic radiation by resonant atoms. When both processes are perfectly balanced, the state of the medium after USP propagates through it coincides with its initial state, and in this sense the medium is transparent. The group velocity of such a stationary USP, called a 2π pulse or a SIT soliton, is smaller than the phase velocity of light in the medium and depends on the pulse duration: The shorter the pulse, the greater is its propagation velocity [3–6]. The shape and group velocity of 2π pulses, as is typical for solitons, do not change. McCall and Hahn were the first to describe and experimentally observe the SIT phenomenon [7]. The fundamental property of the SIT and SIT solitons has been studied many times, both theoretically and experimentally [3,5,6,8]. The SIT phenomenon is of threshold character: The ensemble of two-level absorbers becomes transparent for pulses with areas exceeding a critical value equal to π, where the total area of the pulse is

$$\theta = \frac{2d}{\hbar}\int_{-\infty}^{\infty} E(z,t)dt.$$

Moreover, the propagating pulse area obeys the area theorem [3]. For phase-modulated pulses the area theorem has been presented in [9]. The SIT solitons have been observed experimentally in doped crystals (beginning with ruby [7]), alkali-metal vapors [8], molecular gases (SF_6 [10], NH_3 [11], etc.), iodine vapors [12], semiconductors [13], and nanostructures [14]. Self-transparency was observed in NH_3 at upper vibration-rotational transitions. Inherent for gases, the degeneracy of resonant levels due to arbitrary orientations of the total angular momentum can lead to unusual behavior of solitons. So, for Q-branch transitions with $j = 2$ the resonant transition (fivefold degenerate levels) steady-state pulse profile is a double-humped one, which is a soliton solution of double sine-Gordon equation [15]. It is worth adding that in dense two-level media the near-dipole-dipole interaction modifies the soliton form [16].

*olkhas65@gmail.com

The spatiotemporal dynamics of a light pulse injected into a dense two-level medium under near-dipole-dipole interaction conditions was analyzed in [17]. Two regimes for a soliton, coherent and incoherent, were revealed. In the latter case, the dephasing process is suppressed by dipole-dipole interatomic interaction. Not only are one-soliton solutions found but also a powerful pulse splitting into separate solitons is observed. It has been shown that group-velocity dispersion and diffraction of tilted pulses may make incoherent soliton formation easier.

The account of both resonant and Kerr nonlinearities is especially important for problems of USP propagation in doped fibers. As the authors [18] have shown, in this case the SIT soliton should be also a nonlinear Schrödinger (NLS) soliton of the NLS equation. In other words, such 2π-pulse amplitude and duration should be such that the USP dispersion broadening and its compression due to self-phase modulation exactly compensate each other. The Hirota-type equations were used in papers [19–21] instead of the NLS equation, taking into account the third-order group-velocity dispersion, self-steepening of the pulse edge, and self-induced Raman scattering. The review of works on solitons in media with combined resonant and Kerr nonlinearities can be found in [22]. Local field impact on soliton formation in doped crystals with both types of nonlinearities has been studied in [23], where excitation-induced shift and excitation-induced dephasing were included in the analysis. Soliton implementation is shown to depend on value and sign of pulse carrier frequency detuning from resonance and also on group-velocity dispersion. Inherent both to coherent and incoherent solitons, phase modulation is a function of Kerr nonlinearity and Lorentz frequency.

Successes in the generation of extremely short pulses (few-cycle pulses) by compression or by their direct generation in laser systems have led to the necessity of developing new models describing propagation of such pulses in nonlinear media because often exploited slowly varying envelope approximation (SVEA) is unacceptable for them. A completely integrable model of coherent propagation of such pulses without the SVEA was proposed in [24,25]. If the pulse duration τ_p and resonance transition frequency ω_a obey the condition $\tau_p\omega_a \leqslant 1$, one should use complete Maxwell equations or— under certain conditions—the unidirectional wave approximation [26]. In [26] it has been shown that the propagation of polarized USP in a resonant medium can be described by a two-component generalized modified Korteweg–de Vries equation, which is reduced to a completely integrable equation only in the case of fixed pulse polarization. The authors of [27–29] have proposed another approach to extremely short pulse dynamics analysis. The theory of extremely short solitons in a multilevel medium taking into account all possible transitions with a common level is developed in [30]. It is shown that the dynamics of video pulses is described by a double sine-Gordon equation. The conditions of 0π-, 2π-, and 4π-video-soliton formation have been revealed.

Effects of multifrequency pulse propagation in multilevel media, including soliton solutions, are very diverse and have great potential for many applications. Optical pulse propagation in a three-level medium under two-photon or double one-photon resonance conditions has been extensively studied theoretically and experimentally in connection with SIT, simultaneous different-wavelength optical solitons called simultons [31–33], lasing without inversion [34,35], phaseonium [36], and electromagnetically induced transparency (EIT) [37,38]. As it is shown in [37] under EIT conditions when an arbitrary shaped pulse is applied to an ensemble of population-trapped atoms, the atoms will generate a matching pulse shape on complementary transition. After a certain distance this medium becomes transparent. In contrast to the identical envelopes of EIT matched pulses, adiabatons are predicted in [39] to have the opposite character-complementary envelopes. Adiabatons are generated from initially nonideal pulses after a characteristic propagation distance. The assumption of fully adiabatic behavior is a key condition. The model developed is exactly integrable.

The possibility of simulton lossless propagation in the three-level medium was first predicted in [40]. It is a striking example of the light control by light in a nonlinear medium. To date, there are quite a lot of works devoted to different aspects of simulton formation [41–43]. New multisimulton solutions in three-level systems have been found in [44]. Studies [45,46] have demonstrated that the system of equation governing the evolution of USP in the case of V and Λ configurations are completely integrable and may be solved by use of an inverse scattering transform method. Dynamics of simultons under multiple resonance conditions was studied in [47–49]. According to [50,51], the simultons can be regarded as two-color breathers. Therefore, as in any completely conservative system, the collision of simultons only alters their phase. At the same time, the collision process of two counterpropagating pulses in a degenerate three-level medium can initiate additional simulton birth if the individual pulses are resonant (or near resonant) with the transitions and have orthogonal relative polarizations [52]. Rigorous SIT theory and properties of polarized solitons in the three-level medium under double resonance have been presented in [53] and [54], correspondingly. In [55] the authors have found a solitonlike pulse pair solutions for inhomogeneously broadened Λ- and V-type three-level media. The propagation of simultons has been generalized by Hioe to the propagation of $(N-1)$ pulses in an absorbing N-level medium including cascade configuration under certain conditions for level populations [56].

In works [51,57] more general cases of interaction of two different frequency pulses with the three-level medium in the presence of stationary radiation resonant to the transition between the intermediate and upper levels are analyzed. It is shown, for instance, that at low illumination intensity the first pulse resonant to lower transition is a two-humped one which consists of two pulses with areas approximately equal to 2π. The transient problems associated with such propagations are reviewed in [51].

Hereafter, we study the propagation of two-color ultrashort terahertz (THz) pulses in ammonia vapors. The THz spectral range has attracted much attention of scientists because of its importance in many fields, such as biomedical diagnostics, fingerprint spectroscopy, environment monitoring, security systems, characterization of complex molecules, nanostructures, metamaterials, etc. [58–63]. Although problems in efficient generation and detection of THz radiation still exist, currently this spectral region is being quickly mastered due to the appearance of new sources and detectors of THz waves.

Among the THz sources one can mention free-electron lasers, optical parametric oscillators, quantum-cascade lasers [64], and dipole antennas [65], Nowadays, a lot is being done in order to discover new mechanisms of pulsed THz radiation. The most significant ones are optical rectification of femtosecond pulses in noncentrosymmetric crystals, i.e., GaAs or ZnTe [66], and femtosecond filamentation in gases [67]. Since the THz frequency range corresponds to the spectral width of femtosecond pulses, femtosecond lasers are widely used to generate broadband single-cycle THz waves [68]. However, many applications such as THz time-domain spectroscopy often require predetermined THz pulse shape. The evolution of shaping techniques is nowadays making it possible to generate THz pulses with a given shape and width [69].

Being interested in methods of nonlinear THz spectroscopy of molecular gases, below we analyze the interaction of two THz pulses with the lowest vibration-rotational transitions in ammonia vapor. We demonstrate that in this vapor one can achieve the lossless propagation of simultaneous different-wavelength pulses resonant with different multiplets. The paper is arranged as follows. In Sec. II, we describe the rotation-inversion transitions in ammonia vapors. In Sec. III, we set the equations governing the propagation of two THz optical pulses resonant with lowest rotational levels. Sections IV and V represent Bloch-Maxwell equations in dimensionless form for coupled three- and two-level systems, as well as appropriate conservation laws, correspondingly. In Sec. VI, different simultons that result from this set of equations are given and discussed. Finally, Sec. VII is the conclusion.

II. ROTATION-INVERSION TRANSITIONS IN AMMONIA VAPORS

In this section we briefly mention the main features of the rotation-inversion transitions in ammonia and some results of Ref. [66] necessary for estimating THz pulse propagation in this medium. As known, ammonia is a symmetric top molecule having an oblate form [70] with its moment of inertia along the principal axis smaller than the one along the symmetry axis (z axis). Each rotational state with angular momentum $\mathbf{P}$ is uniquely determined by a pair of quantum numbers: the rotational quantum number J and the projection quantum number K, where $K = J, J-1, \ldots, -J$.

Moreover, for each (J,K) level, with $K > 0$, two states of symmetry, $+$ and $-$, can be distinguished, related to the symmetry of the rotational wave functions. These states of symmetry (inversion states) are associated with the nitrogen atom position relative to the symmetry plane, defined by the three hydrogen atoms. THz radiation excites the lowest rotational transitions of the vibration ground state, obeying the following selection rules: $+ \leftrightarrow -$, $\Delta J = 0, \pm 1$, and $\Delta K = 0$, as indicated in Fig. 1 [66,70]. For values of $K \neq 0$, the inversion transitions $+ \leftrightarrow -$ obey the following selection rules: $\Delta J = 0, \Delta K = 0$. For ammonia, the inversion frequency is $\omega_{0i}/2\pi = 23.8$ GHz [70].

The authors of [63] note for ammonia molecules a slight anharmonicity in the line spacing of the rotational lines and the removal of the K degeneracy. In addition, the inversion lines are also nondegenerate, but spread over a spectral interval of about 10 GHz.

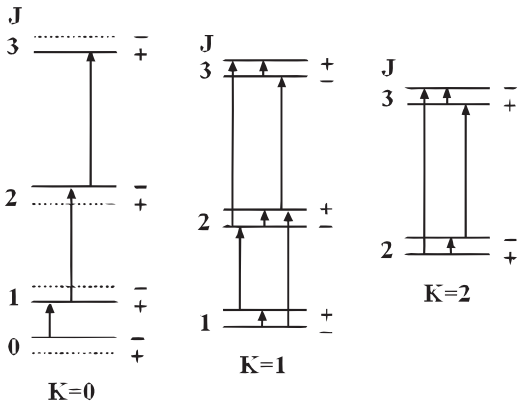

FIG. 1. Level scheme of ammonia indicating the inversion and rotation transitions, taken from Ref. [66].

For $J > 0$, one can distinguish two components for a rotational line, with frequencies

$$\frac{\omega_r^{\pm}(J)}{2\pi} = 2\bar{J}(B_v - D_{JK}\bar{K}^2) - 4D_J\bar{J}^3 \pm \frac{\omega_i}{2\pi}. \quad (1)$$

Here $\bar{J} = J + 1$, B_v is the rotational constant of the vibrational ground state; D_J and D_{JK} are the respective centrifugal stretching constants [71]. $\bar{K}$ is an average value of the quantum number K accounting for all K transitions with the same quantum number J. As shown in [66], at low pressures the ammonia spectrum comprises individual K transitions belonging to the same quantum number $J > 0$ and reveals dependence of their widths on the quantum numbers J and K. At pressures of 1000 hPa and higher, absorption bands of ammonia consist of individual well-resolved lines, which depend only on J. These lines are an average over all K transitions. For example, for 2000 hPa the lowest rotational lines, respectively, lie in the region 0.6, 1.2, 1.7 THz [66], etc. (Fig. 2). As the pressure builds up, absorption lines are broadened, but their intensity does not increase.

Hereafter, we consider the nonlinear interaction of THz pulses with ammonia vapor. The results of this process

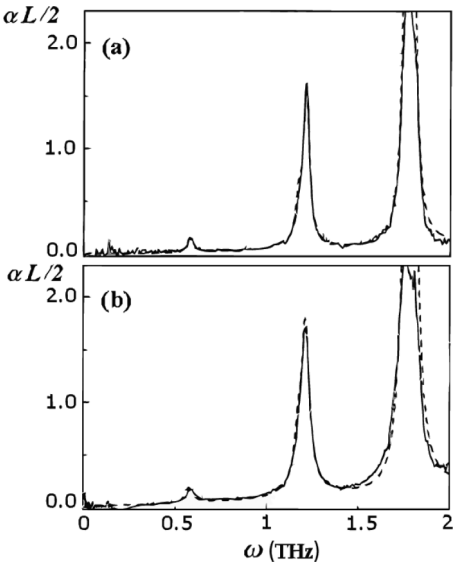

FIG. 2. Absorption spectrum of ammonia for (a) 200 hPa and (b) 2950 hPa, taken from Ref. [66]; $\alpha L/2$ is the dimensionless absorption.

essentially depend on gas cell length, vapor pressure, and temperature, as well as on the resonance conditions, intensity, and spectral width of the input pulse. For instance, the result of the pulse propagation in ammonia vapor will strongly depend on the THz pulse duration. The propagation of a one-cycle THz pulse whose spectral width overlaps many transitions of ammonia is largely different from the propagation of a long enough pulse that is resonant to a single transition.

It is important to notice that the traditionally used SVEA is not valid for extremely short (one-cycle) THz pulses. Hereafter, we present and discuss the simultaneous propagation of two long-enough THz pulses in an extended ammonia cell. We consider that the pulses are resonant with lowest rotational transitions of ammonia. More precisely, the transitions considered are the following: for $K = 0$, $- \leftrightarrow +$, $J = 0 \leftrightarrow 1$ and $+ \leftrightarrow -$, $J = 1 \leftrightarrow 2$ and for $K = \pm 1$, $J = 1 \leftrightarrow 2$, $+ \leftrightarrow -$ and $- \leftrightarrow +$. One of the THz pulses is resonant with the lowest transition of the three-level system, and the other one is resonant with both the upper transition of the three-level system and four two-level systems. Under these approximations, the problem reduces to the investigation of two shaped THz pulses that propagate in a medium with two different multiplets: three- and two-level subsystems.

III. NONREDUCED BLOCH-MAXWELL EQUATIONS FOR COUPLED THREE- AND TWO-LEVEL SYSTEMS

Let us now consider the interaction of the two copropagating and nondegenerate-in-frequency THz pulses $E_1(t)$ and $E_2(t)$ that propagate in a molecular medium consisting of three- and two-level subsystems. These pulses are assumed to have a duration long enough to ensure that the concept of a carrier frequency is valid. As we already mentioned, the first THz pulse at the carrier frequency $\omega_1 \approx 0.6$ THz is resonant with the transition $K = 0, - \leftrightarrow +$, $J = 0 \leftrightarrow 1$, while the second one with the frequency $\omega_2 \approx 1.2$ THz is in resonance with both the upper transition of the three-level ($K = 0$, $+ \leftrightarrow -$, $J = 1 \leftrightarrow 2$) and the two-level systems ($K = \pm 1$, $+ \leftrightarrow -$, $J = 1 \leftrightarrow 2$) (see Fig. 1). We focus on the coherent regime of interaction of both pulses with the medium assuming that their durations are less than the phase and population relaxation times. Then the associated Maxwell-Bloch equations are the following:

$$\frac{d\rho_{10}}{dt} = -i\omega_{10}\rho_{10} + \frac{i}{\hbar}d_{10}E_1 n_{10} + \frac{i}{\hbar}d_{21}E_2^*\rho_{20}, \tag{2}$$

$$\frac{d\rho_{21}}{dt} = -i\omega_{21}\rho_{21} + \frac{i}{\hbar}d_{21}E_2 n_{21} - \frac{i}{\hbar}d_{10}E_1^*\rho_{20}, \tag{3}$$

$$\frac{d\rho_{20}}{dt} = -i\omega_{20}\rho_{20} + \frac{i}{\hbar}d_{21}E_2\rho_{10} - \frac{i}{\hbar}d_{10}E_1\rho_{21}, \tag{4}$$

$$\frac{dn_{10}}{dt} = -\frac{2i}{\hbar}d_{10}(E_1\rho_{01} - E_1^*\rho_{10}) - \frac{i}{\hbar}d_{21}(E_2^*\rho_{21} - E_2\rho_{12}), \tag{5}$$

$$\frac{dn_{21}}{dt} = -\frac{2i}{\hbar}d_{21}(E_2\rho_{12} - E_2^*\rho_{21}) - \frac{i}{\hbar}d_{10}(E_1^*\rho_{10} - E_1\rho_{01}), \tag{6}$$

$$\frac{d\rho_{21}^l}{dt} = -i\omega_{21}^l\rho_{21}^l + \frac{i}{\hbar}d_{21}^l E_2 n_{21}^l, \tag{7}$$

$$\frac{dn_{21}^l}{dt} = -\frac{2i}{\hbar}d_{21}^l\left(E_2\rho_{21}^l - E_2^*\rho_{12}^l\right), \tag{8}$$

$$\Delta E_i - \mu_0\frac{\partial^2 D_i}{\partial t^2} = 0. \tag{9}$$

Here Eqs. (2)–(6) and (7) and (8) are the Bloch equations set for three-level and two-level systems, respectively; ρ_{ij} is the ijth density matrix element of the three-level system and ρ_{ij}^l is the ijth density matrix element of the lth two-level system, $l = 1$–4; $n_{ij} = \rho_{ii} - \rho_{jj}$ and $n_{ij}^l = \rho_{ii}^l - \rho_{jj}^l$, $\hbar\omega_{ij}^l$ and $\hbar\omega_{ij}$, and d_{ij} and d_{ij}^l are, respectively, the population differences, energy, and dipole moments of actual transitions. The nonlinear evolution of both pulses is described by the wave equation (9), which is presented in SI units, where μ_0 is the magnetic constant, E_i and D_i are the THz field amplitude and the electric displacement, respectively, at frequency ω_i. Here $\omega_1 \approx \omega_{10}$ and $\omega_2 \approx \omega_{21}$. The electric displacement in the dielectric medium is linked to the external field E and the induced polarization P by the relation $D = \varepsilon_0 E + P$, where ε_0 is the electric constant and the polarization P includes linear $P_{lin}(\omega_i) = \varepsilon_0\chi(\omega_i)E_i$ and nonlinear P_{nl} components; $\chi(\omega_i)$ is the electric susceptibility. At resonance, the nonlinear macroscopic polarization induced by the two THz pulses equals the sum of $P_1 = N\{\rho_{01}d_{10} + \rho_{10}d_{01}\}$ at frequency ω_1 and $P_2 = N\{\rho_{12}d_{21} + \rho_{21}d_{12} + \sum_{l=1}^{4}(\rho_{12}^l d_{21}^l + \rho_{21}^l d_{12}^l)\}$ at frequency ω_2. Substituting these expressions into the Eq. (9), one obtains the wave equation

$$\Delta E_i - \frac{n_i^2}{c^2}\frac{\partial^2 E_i}{\partial t^2} = \mu_0\frac{\partial^2 P_i}{\partial t^2}, \tag{10}$$

where $c^2/n_i^2 = [(1+\chi)\varepsilon_0\mu_0]^{-1}$, n_i being the refractive index of the medium and c/n_i the phase velocity of the THz pulse at frequency ω_i. Equations (2)–(10) govern the copropagation of two-color THz pulses at their coherent interaction with the medium as well as pulse widths being short relative to molecular relaxation times. This set of equations is unlikely to be integrated. If only one resonant THz pulse passes through the medium, our task is reduced to a two-level model, and the Maxwell-Bloch equations are integrable in both reduced and nonreduced form [72]. In the latter case, the only approximation used is the approximation of unidirectional waves [26,73]. The reduced Maxwell-Bloch equation set in the two-level limit can describe a SIT phenomenon originating from a balance of the absorption and re-emission of electromagnetic radiation by resonant atoms of the medium in such a manner that a steady-state optical pulse propagates. In this meaning the medium is transparent. The group velocity of such a steady-state pulse, called 2π pulse or SIT soliton, is less than the phase speed of light in the medium. The group velocity depends on the 2π-pulse duration: The shorter the duration, the higher is its speed [3,5]. The solitons keep their shape and velocity under propagation and after collisions. From a mathematical point of view, this property is a consequence of the complete integrability of the reduced Maxwell-Bloch equations [22,74]. The very 2π pulse is the single-soliton solution of these equations. In general, all other parameters of solitons may alter. Fundamental properties of the SIT solitons have been studied many times, both theoretically and experimentally [3–10].

In the absence of two-level subsystems the equation system presented above is reduced to a model of copropagation of two USPs in a three-level medium with cascade transitions. While this problem is not integrable, it makes it possible to obtain analytic solutions at appropriate relations between the pulse amplitudes, frequencies, and the dipole moments of corresponding transitions and it is feasible to trap two pulses by a simulton [31,47].

IV. DIMENSIONLESS BLOCH-MAXWELL EQUATIONS FOR COUPLED THREE- AND TWO-LEVEL SYSTEMS

Now let us focus on the propagation of two shaped pulses containing a sufficiently large number of cycles in the above molecular medium. Strictly speaking, the four two-level systems for $K = \pm 1$ are not independent, since they are coupled via inverse transitions, which lie in gigahertz range of the spectrum [see Fig. 1 and Eq. (1)]. Note that the pulse durations available in the future experiment should fit with the SVEA. Such pulses will not have gigahertz spectral components in their spectra to excite the inverse transitions. Therefore, we will suppose that all two-level subsystems interact with the second THz pulse independently from each other. In addition, the second pulse is assumed to be in resonance with the upper transition of the three-level subsystem and with all two-level subsystems. Let us introduce new variables $\rho_{01} = \bar{\rho}_{01}e^{i\omega_1 t}$, $\rho_{12} = \bar{\rho}_{12}e^{i\omega_2 t}$, $\rho_{02} = \bar{\rho}_{02}e^{i(\omega_1+\omega_2)t}$, $\rho_{ij} = \rho^*_{ji}$. Supposing that both THz pulses are quasimonochromatic plane waves copropagating along the z axis, i.e., $\vec{E}_i(z,t) = \vec{e}\mathcal{E}_i(z,t)e^{i(\omega_i t - k_i z)} + \text{c.c.}$, $i = 1,2$, within the scope of the SVEA the Maxwell-Bloch equations are transformed into the reduced form:

$$\frac{d\bar{\rho}_{01}}{dt} = i\delta_{01}\bar{\rho}_{01} - \frac{i}{\hbar}(d_{01}\mathcal{E}_1 n_{01} + d_{21}\mathcal{E}_2^*\bar{\rho}_{02}), \tag{11}$$

$$\frac{d\bar{\rho}_{12}}{dt} = i\delta_{12}\bar{\rho}_{12} - \frac{i}{\hbar}(d_{12}\mathcal{E}_2 n_{12} - d_{10}\mathcal{E}_1^*\bar{\rho}_{02}), \tag{12}$$

$$\frac{d\bar{\rho}_{02}}{dt} = i(\delta_{01}+\delta_{12})\bar{\rho}_{02} + \frac{i}{\hbar}(d_{01}\mathcal{E}_1\bar{\rho}_{12} - d_{12}\mathcal{E}_2\bar{\rho}_{01}), \tag{13}$$

$$\frac{d\rho_{00}}{dt} = \frac{i}{\hbar}(d_{01}\mathcal{E}_1\bar{\rho}_{10} - d_{10}\mathcal{E}_1^*\bar{\rho}_{01}), \tag{14}$$

$$\frac{d\rho_{11}}{dt} = \frac{i}{\hbar}(d_{10}\mathcal{E}_1^*\bar{\rho}_{01} - d_{01}\mathcal{E}_1\bar{\rho}_{10}) + \frac{i}{\hbar}(d_{12}\mathcal{E}_2\bar{\rho}_{21} - d_{12}\mathcal{E}_2^*\bar{\rho}_{12}), \tag{15}$$

$$\frac{d\rho_{22}}{dt} = \frac{i}{\hbar}(d_{21}\mathcal{E}_1^*\bar{\rho}_{12} - d_{12}\mathcal{E}_2\bar{\rho}_{21}), \tag{16}$$

$$\frac{d\bar{\rho'}_{12}}{dt} = i\delta'_{12}\bar{\rho'}_{12} - \frac{i}{\hbar}d'_{12}\mathcal{E}_2 n', \tag{17}$$

$$\frac{dn'}{dt} = \frac{2i}{\hbar}(d'_{12}\mathcal{E}_2\bar{\rho'}_{21} - d'_{21}\mathcal{E}_2^*\bar{\rho'}_{12}), \tag{18}$$

$$\frac{\partial\mathcal{E}_1}{\partial z} + \frac{n_1}{c}\frac{\partial\mathcal{E}_1}{\partial t} = -i\frac{\mu_0\omega_1 cNd_{01}}{2n_1}\bar{\rho}_{01}, \tag{19}$$

$$\frac{\partial\mathcal{E}_2}{\partial z} + \frac{n_2}{c}\frac{\partial\mathcal{E}_2}{\partial t} = -i\frac{\mu_0\omega_2 cN}{2n_2}(d_{21}\bar{\rho}_{12} + 4d'_{21}\bar{\rho'}_{12}). \tag{20}$$

Here $\delta_{01} = \omega_{10} - \omega_1$, $\delta_{12} = \omega_{21} - \omega_2$, $\delta_{ij} = -\delta_{ji}$, $\delta_{01}(\delta_{12})$ is the first (second) pulse frequency detuning from the lower (upper) transition frequency and δ'_{12} is the frequency detuning of the last pulse from resonance with the two-level system. One can see that, for both THz fields, the two cascade transitions in the three-level subsystem and the four two-level subsystems are not independent. First, the transitions $0 \leftrightarrow 1$ and $1 \leftrightarrow 2$ compete for the population of level 1 through their interaction with the THz pulses. Second, the superposition of the states $|0\rangle$ and $|2\rangle$ occurs owing to simultaneous action of both THz pulses. Finally, the three-level subsystem and four two-level subsystems are coupled via the pulse $\mathcal{E}_2$. Since all two-level systems differ little from each other in frequencies and in transition dipole moments, they are supposed to be identical. Therefore, instead of matrix elements $\rho^l_{21(12)}$ and n^l_{21} we have introduced in Eqs. (17) and (18) $\rho'_{21(12)}$ and n' in order to describe two-level systems.

In new variables, the equation set (11)–(20) can be written in a dimensionless form,

$$\frac{d\bar{\rho}_{01}}{d\tau} = i\delta_1\bar{\rho}_{01} - iE_l n_{01} - iE_2^*\bar{\rho}_{02}, \tag{21}$$

$$\frac{d\bar{\rho}_{12}}{d\tau} = i\delta_2\bar{\rho}_{12} - iE_2 n_{12} + iE_1^*\bar{\rho}_{02}, \tag{22}$$

$$\frac{d\bar{\rho}_{02}}{d\tau} = i\left(\delta_1+\delta_2\right)\bar{\rho}_{02} + i\left(E_1\bar{\rho}_{12} - E_2\bar{\rho}_{01}\right), \tag{23}$$

$$\frac{d\rho_{00}}{d\tau} = i(E_1\bar{\rho}_{10} - E_1^*\bar{\rho}_{01}), \tag{24}$$

$$\frac{d\rho_{11}}{d\tau} = i[(E_1^*\bar{\rho}_{01} - E_1\bar{\rho}_{10}) + (E_2\bar{\rho}_{21} - E_2^*\bar{\rho}_{12})], \tag{25}$$

$$\frac{d\rho_{22}}{d\tau} = i(E_2^*\bar{\rho}_{12} - E_2\bar{\rho}_{21}), \tag{26}$$

$$\frac{d\bar{\rho}'_{12}}{d\tau} = i\delta\bar{\rho}'_{12} - i\sigma E_2\bar{n}'_{12}, \tag{27}$$

$$\frac{dn'}{d\tau} = 2i(E_2\bar{\rho}'_{21} - E_2^*\bar{\rho}'_{12}), \tag{28}$$

$$\varkappa\frac{dE_1}{d\tau} = i\bar{\rho}_{01}, \tag{29}$$

$$\varkappa\frac{dE_2}{d\tau} = i\lambda^2(\bar{\rho}_{12} + 4\sigma\bar{\rho}'_{12}), \tag{30}$$

where $E_i = d_{i1}\mathcal{E}_i/\hbar\omega_p$; $\delta_i = \delta_{i-1,i}/\omega_p$; $\delta = \delta'_{12}/\omega_p$; $\tau = \omega_p(t - z/v)$; $\xi = z\cdot\omega_p n/c$; $\omega_p^2 = \mu_0\omega_1 c^2 N d_{i1}^2/(2\hbar n_0^2)$; $\lambda^2 = (d_{12}^2/d_{01}^2)(\omega_2/\omega_1)$; $\varkappa = [c/(nv) - 1]$; $\sigma = d'_{12}/d_{12}$, where v is the group velocity. We have introduced the automodel variable τ being interested in steady-state solutions for both THz pulses.

V. CONSERVATION LAWS

As mentioned above, the problem under investigation is unlikely to be integrable, but we may find a solution by use of appropriate conservation laws for the set of Eqs. (21)–(30). Multiplying Eq. (29) by E_1^* and the corresponding complex conjugate equation by E_1 and then summing them, we obtain,

taking into account (24), the first conservation law,

$$\varkappa |E_1|^2 = \left(\rho_{00}^0 - \rho_{00}\right), \tag{31}$$

where ρ_{00}^0 is the initial population of the lower level of the three-level system. As follows from this law, the first pulse intensity is associated with a change of the population of the lower level of the three-level system.

In a similar way we can deduce a second conservation law using Eq. (30) and its conjugate. This law binds the second pulse intensity with changes of the upper level population of the three-level system and the population difference of the two-level ones:

$$\varkappa |E_2|^2 = \left(\rho_{22} - \rho_{22}^0\right) + 2(n_0' - n'). \tag{32}$$

Three additional conservation laws can be derived from the properties of the actual resonant systems,

$$\rho_{00} + \rho_{11} + \rho_{22} = \text{const}, \tag{33}$$

$$v_{01}^2 + v_{12}^2 + u_{02}^2 + 2\left(\rho_{00}^2 + \rho_{11}^2 + \rho_{22}^2\right) = \text{const}, \tag{34}$$

for the three-level system [31], where

$$u_{ij} = (1/2)(\bar{\rho}_{ij} + \bar{\rho}_{ji}), v_{ij} = (1/2)(\bar{\rho}_{ij} - \bar{\rho}_{ji})$$

and

$$4\bar{\rho}_{12}'\bar{\rho}_{21}' + (n')^2 = \text{const} \tag{35}$$

for the two-level one. The expression (33) is the total probability conservation law. As for Eqs. (34) and (35), they express the conservation of the length of the Bloch vector in the three- and two-level subsystems. With conservation laws (31)–(33) we can obtain a relation between population variation of the intermediate level, intensities of the two propagating pulses, and population differences of all excited two-level subsystems:

$$\varkappa |E_1|^2 - \varkappa |E_2|^2 / \lambda^2 = 2(n_0' - n') + \left(\rho_{11} - \rho_{11}^0\right). \tag{36}$$

One can see that its variation depends on energy exchange between both pulses and the two-level subsystems. When such energy exchange is balanced, ρ_{11} remains constant during pulse propagation.

It is worth noting that the search for solutions does not become an easy problem even with the conservation laws derived above, because all components of the THz fields, polarizations, and level populations are interconnected. As can be seen from Eq. (25), level 1 is involved in energy exchange between the both THz pulses and the three-level system. In its turn, the second pulse intensity depends on energy exchange with the two-level subsystems. Polarizations for the two adjacent transitions, as evident from Eqs. (21) and (22), are related to each other through a superposition state of lower and upper levels. Therefore, it is difficult to advance in this way without additional conditions or hypotheses. Such conditions as coherent population trapping or adiabatic population transfer [75], supposing that the intermediate level population keeps its initial value $\rho_{11} = \rho_{11}^0$ and does not vary under traveling of the THz pulses through the medium, make it possible to simplify the problem under study substantially. This approximation is justified for balanced energy exchange between pulses and two-level subsystems. In this case, one more conservation law relating both THz fields to each other and to population difference of the four two-level subsystems is satisfied:

$$\varkappa |E_1|^2 = \frac{\varkappa |E_2|^2}{\lambda^2} + 2(n_0' - n'). \tag{37}$$

The set of Eqs. (21)–(30) in combination with the conservation laws (31)–(35) allows us to derive equations for E_1 and E_2. Differentiating Eq. (29) with respect to τ and substituting into Eq. (21) we arrive at

$$-\varkappa \ddot{E}_1 = \delta_1 \bar{\rho}_{01} - E_1 (\rho_{00} - \rho_{11}) - E_2^* \bar{\rho}_{02}. \tag{38}$$

Before we get the equations for the field envelopes, let us find out the relation between their phases. To this end, we transform (38), inserting within it the value ρ_{02} defined via Eq. (22). Using (29)–(32) and also (36) we obtain

$$\begin{aligned}
&\varkappa \ddot{E}_1 E_1^* + \frac{\varkappa \ddot{E}_2 E_2^*}{\lambda^2} \\
&= i\left(\delta_1 \dot{E}_1 E_1^* + \frac{\varkappa \delta_2 \dot{E}_2 E_2^*}{\lambda^2} + 4\sigma E_2^* \dot{\bar{\rho}}_{12}'\right) \\
&\quad + |E_1|^2 \left(\rho_{00}^0 - \rho_{11}^0 - 2n_0' - 2\varkappa |E_1|^2 + \frac{\varkappa |E_2|^2}{\lambda^2} + 2n'\right) \\
&\quad + |E_2|^2 \left(\rho_{11}^0 - \rho_{22}^0 + 4n_0' + \frac{\varkappa |E_1|^2 - 2\varkappa |E_2|^2}{\lambda^2} - 4n'\right) \\
&\quad + 4\sigma \delta_2 E_2^* \bar{\rho}_{12}'.
\end{aligned}$$

Assuming that

$$E_i(\tau) = A_i(\tau) \exp\{i\varphi_i(\tau)\}, \tag{39}$$

with $i = 1,2$, one can get the equation for the phases of both fields from the imaginary part of the last equation:

$$\begin{aligned}
&\varkappa A_1 (2\dot{A}_1 \dot{\varphi}_1 + A_1 \ddot{\varphi}_1) + \varkappa A_2 (2\dot{A}_2 \dot{\varphi}_2 + A_2 \ddot{\varphi}_2)/\lambda^2 \\
&\quad = \varkappa \delta_1 \dot{A}_1 A_1 + \varkappa \delta_2 \dot{A}_2 A_2 / \lambda^2 - 2\sigma(\delta_2 - \delta) n_0' A_2 \sin\theta_2.
\end{aligned} \tag{40}$$

Here $\theta_2(\tau) = 2\sigma \int_{-\infty}^{\tau} A_2 dt$ is the second pulse area. Equation (40) may be integrated from $t = \infty$ to $t = \tau$ in order to yield

$$\begin{aligned}
\varkappa A_1^2 \dot{\varphi}_1 - \varkappa \delta_1 A_1^2/2 &= -\varkappa A_2^2 \dot{\varphi}_2/\lambda^2 + \varkappa A_2^2/(2\lambda^2) \\
&\quad + (\delta_2 - \delta) n_0' (\cos\theta_2 - 1).
\end{aligned} \tag{41}$$

It is evident that the three- and two-level systems contribute to the phase modulation of the second pulse. However, when its carrier frequency is detuned from resonance in such a way that $\delta_2 = \delta$, the influence of two-level subsystems disappears and both pulses obey the modulation law inherent to SIT [5]. It is easy to show that, in the stationary case [76], the phase modulation rate varies in accordance with

$$\dot{\varphi}_i = c_i / A_i^2. \tag{42}$$

The phase modulation constant C_i may be nonzero only for periodic pulse trains. For a solitary wave $C_i = 0$, in other words, the pulse solutions are not phase modulated.

Below we show that two THz pulses of appropriate initial forms and intensities may be trapped in a coupled state like simulton and propagate in ammonia vapor basically with no distortions.

VI. COUPLED STATES OF TERAHERTZ SOLITARY WAVES

Let us focus on searching for possible scenarios of distortionless propagation in ammonia vapors of two THz pulses trapped by a simulton. As it is known, the simulton concept was introduced [31] for a pair of two unidirectional short pulses propagating in a three-level medium with cascade transitions, which form a steady coupled state. It was shown [46,47] that two solitons in a medium with equal oscillator strengths of the adjacent transitions can be trapped into a simulton provided that the level populations are preliminarily prepared. The problem of a THz simulton formation in ammonia vapors is different. On one hand, all relevant levels are populated at room temperature and the necessary conditions of level population pretreatment are removed. On the other hand, the presence of two-level subsystems certainly influences the problem of trapping the terahertz pulses in a simulton state.

So, searching for stationary solutions, we suppose that both pulses are not phase modulated, viz., $\varphi_1 = \varphi_2 = \text{const}$, and the exact resonance conditions are provided. Then the Bloch-Maxwell equations (21)–(30) are reduced to

$$\dot{v}_{01} = 2A_1(\rho_{00} - \rho_{11}) + A_2 u_{02}, \tag{43}$$
$$\dot{v}_{12} = 2A_2(\rho_{11} - \rho_{22}) - A_1 u_{02}, \tag{44}$$
$$\dot{u}_{02} = A_1 v_{12} - A_2 v_{01}, \tag{45}$$
$$\dot{\rho}_{00} = -A_1 v_{01}, \tag{46}$$
$$\dot{\rho}_{11} = A_1 v_{01} - A_2 v_{12}, \tag{47}$$
$$\dot{\rho}_{22} = A_2 v_{12}, \tag{48}$$
$$\dot{v}' = 2\sigma A_2 n', \tag{49}$$
$$\dot{n}' = -2\sigma A_2 v', \tag{50}$$
$$2\varkappa \dot{A}_1 = v_{01}, \tag{51}$$
$$2\varkappa \dot{A}_2/\lambda^2 = v_{12} + 4\sigma v', \tag{52}$$

where $v_{ij} = \frac{1}{2i}(\rho_{ij} - \rho_{ji})$, $u_{ij} = \frac{1}{2}(\rho_{ij} + \rho_{ji})$, $i,j = 0,1,2$. Differentiating Eq. (51) with respect to τ and substituting Eq. (43) lead to

$$-\varkappa \ddot{A}_1 = -A_1(\rho_{00} - \rho_{11}) - A_2 u_{02}. \tag{53}$$

Dividing this equation by A_1 and differentiating it again with respect to τ gives

$$-\varkappa(\dddot{A}_1 A_2 - \ddot{A}_1 \dot{A}_2)/A_2^2 = (\dot{A}_1 A_2 - A_1 \dot{A}_2)(\rho_{00} - \rho_{11})/A_2^2 + A_1(\dot{\rho}_{00} - \dot{\rho}_{11})/A_2 + \dot{u}_{02}.$$

Further substituting (45)–(47), (31), and (36) into this last equation and using Eqs. (51) and (52) we obtain

$$\varkappa \frac{\dddot{A}_1 A_2 - \ddot{A}_1 \dot{A}_2}{A_2^2} = \frac{\dot{A}_1 A_2 - A_1 \dot{A}_2}{A_2^2}\left(\rho_{00}^0 - \rho_{11}^0 - 2\varkappa A_1^2 - 2n_0' + \varkappa A_2^2/\lambda^2 + 2n'\right) + \frac{2A_1}{A_2}(-2\varkappa \dot{A}_1 A_1 + \dot{n}') + \varkappa \dot{A}_2 A_1/\lambda^2 - \varkappa \dot{A}_1 A_2 - 4\sigma A_1 v.' \tag{54}$$

According to Eq. (54), the two-level systems affect the first pulse despite the fact that it is not resonant with them. Their contribution can be easily obtained from the solutions of Eqs. (49) and (50): $n' = n_0' \cos\theta_2$, $v' = n_0' \sin\theta_2$. Then Eq. (54) reduces to

$$\varkappa(\dddot{A}_1 A_2 - \ddot{A}_1 \dot{A}_2) - (\dot{A}_1 A_2 - A_1 \dot{A}_2) \times \left(\rho_{00}^0 - \rho_{11}^0 - 2n_0' - 2\varkappa A_1^2 + \varkappa/\lambda^2 A_2^2 + 2n_0' \cos\theta_2\right) - 2A_1 A_2(-2\varkappa \dot{A}_1 A_1 + \varkappa/\lambda^2 \dot{A}_2 A_2 - 2n_0' \sin\theta_2) - \varkappa/\lambda^2 A_1 A_2^2 \dot{A}_2 + \varkappa \dot{A}_1 A_2^3 + 4n_0' A_1 A_2^3 \cos\theta_2 = 0, \tag{55}$$

where $\sigma = 1$.

To determine the equation for the second field, we differentiate Eq. (52) and substitute (44) and (49) multiplied by 4, which results in

$$\varkappa \ddot{A}_2/\lambda^2 = \dot{v}_{12} + 4\dot{v}' = 2A_2(\rho_{11} - \rho_{22}) + A_1 u_{02} + 8A_2 n'. \tag{56}$$

Repeating a similar procedure as for Eq. (53), Eq. (56) leads to

$$\varkappa(\dddot{A}_2 A_1 - \ddot{A}_2 \dot{A}_1)/\lambda^2 - (\dot{A}_2 A_1 - A_2 \dot{A}_1) \times \left(\rho_{11}^0 - \rho_{22}^0 + 4n_0' + \varkappa A_1^2 - 2\varkappa A_2^2/\lambda^2\right) - 2\varkappa A_1 A_2(\dot{A}_1 A_1 - \dot{A}_2 A_2/\lambda^2) + \varkappa \dot{A}_2 A_1^3/\lambda^2 - \varkappa A_2 \dot{A}_1 A_1^2 - 4n_0' A_1^3 A_2 \cos\theta_2 = 0. \tag{57}$$

Since the integro-differential equation system (55) and (57) can hardly be solved analytically, let us simplify our task and consider the behavior scenarios for the first and the second pulses, propagating independently. Indeed, the first THz pulse resonant with the transition $K = 0$, $- \leftrightarrow +$, $J = 0 \leftrightarrow 1$ or the second pulse, that is in resonance with five nondegenerate transitions ($K = 0$, $+ \leftrightarrow -$, $J = 1 \leftrightarrow 2$, and $K = \pm 1$, $+ \leftrightarrow -$, $J = 1 \leftrightarrow 2$), may propagate as SIT solitons in a two-level system [5] with the hyperbolic secant shape and duration $\tau_{p1} = \sqrt{\varkappa/(\rho_{00}^0 - \rho_{11}^0)}$ or $\tau_{p2} = \sqrt{\varkappa/[5(\rho_{11}^0 - \rho_{22}^0)]}/\lambda$, correspondingly. Obviously, the soliton durations depend on initial populations of resonant levels. We emphasize that, at room temperature, all resonant levels are populated in accordance with the Boltzmann distribution because the photon energy in the THz range is comparable to the thermal energy kT. Compared to the first pulse, the duration of the second soliton is less by a factor $\lambda\sqrt{5}$. The value of the parameter λ may be estimated from the absorption of the medium at 0.6 and 1.2 THz. According to the absorption spectrum, presented in Fig. 2 [66], $\lambda \approx 2$. Both solitons are one humped.

Now we consider solutions for a balanced energy exchange between pulses assuming that $\rho_{11} = \text{const}$ during the passage of both THz pulses through the medium. The validity of the conservation law (37) in this case allows us to simplify essentially Eqs. (55) and (57) reducing them to the form

$$\kappa[2A_1 A_2 \ddot{A}_1 + \dot{A}_1(A_2 \dot{A}_1 - A_1 \dot{A}_2)] = A_2^3(n_{12}^0 - \kappa A_1^2) + A_2 A_1^2(n_{01}^0 - \kappa A_1^2), \tag{58}$$

$$\kappa\left(\frac{1}{\lambda^2} A_2 \ddot{A}_2 + A_1 \ddot{A}_1\right) = A_2^2\left[n_{12}^0 + 2n_0' - \kappa\left(\frac{2}{\lambda^2} A_2^2 - A_1^2\right)\right] + A_1^2(n_{01}^0 - \kappa A_1^2), \tag{59}$$

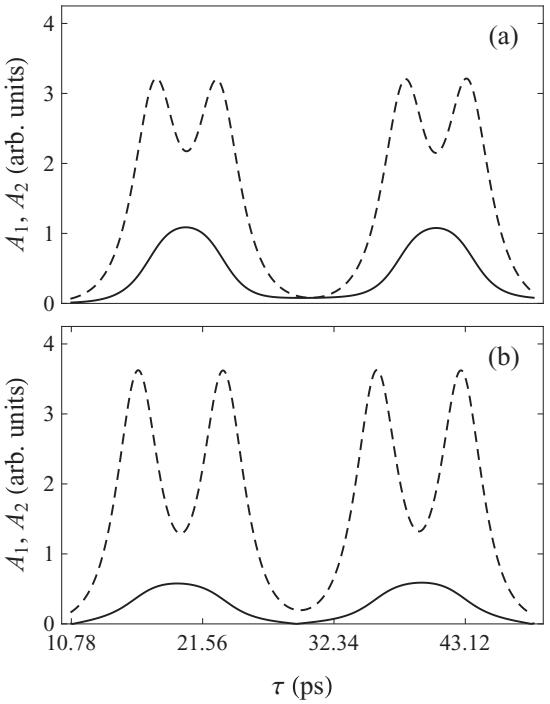

FIG. 3. Coupled wave trains A_1 (solid curve) and A_2 (dashed curve) in dependence on initial conditions: (a) $\rho_{00}^0 = 0.0390$, $\rho_{11}^0 = 0.0379$, $\rho_{22}^0 = 0.0371$; (b) $\rho_{00}^0 = 0.039$, $\rho_{11}^0 = 0.038$, $\rho_{22}^0 = 0.037$.

where $n_{12}^0 = \rho_{11} - \rho_{22}^0$ and $n_{01}^0 = \rho_{00}^0 - \rho_{11}$. By the way, the first results on simultons have been obtained for the three-level medium with the cascade level configuration [31] under the condition $\rho_{11} = \text{const}$. However, unlike them, the level configuration in ammonia vapor is more complicated and the oscillator strength of the upper transition in the three-level subsystem and of two-level ones is twice the value of the lower transition oscillator strength. It makes THz simulton observation in molecular vapors a more difficult problem.

Let us consider some results obtained by a numerical analysis of Eqs. (58) and (59). For nonzero initial values of the amplitude and its first-order derivative for each field, these equations demonstrate a bound state of two periodic waves: an intensive one having a double-humped profile and a weaker wave possessing a one-humped shape [see Fig. 3(a)]. The latter is in resonance with the $0 \leftrightarrow 1$ transition of the three-level subsystem, whereas the more powerful one interacts with the upper transition of the three-level subsystem and the four two-level subsystems. Notice that the more powerful the second wave and the greater the distance between the humps, the weaker is the first one [Fig. 3(b)]. Such a periodic solution can be considered as an infinite sequence of short pulses spreading in a resonant medium free of any dissipation. Since Eqs. (56) and (57) are valid when the wave-packet durations are much smaller than the relaxation times of the molecular medium, they are only mathematical objects. However, in our opinion, it is worth discussing this novel class of stationary solutions as an illustration of the properties of the models under consideration. The same periodic solutions are obtained for the more general case where $\rho_{11} \neq$ const by solving the Bloch-Maxwell equations (43)–(52) numerically.

The solutions presented in Figs. 3(a) and 3(b) are certainly steady bound states of two waves. First, their periods are the same, and second, in the absence of a weak A_1 wave, A_2 becomes a one-hump wave with a shorter period. Moreover, this bound state strongly depends on the initial conditions for both waves. Multihump stationary waves and their structures have been identified earlier and their stability regions have been examined numerically for a Korteweg–de Vries equation with nonlocal perturbation [77] and for a dissipative Benjamin-Ono equation [78]. The relation between the irregular behavior of the initial value problem and the multiplicity of stationary waves has also been revealed. The interaction of two intensive shallow water waves with different wave and phase speeds leads also to double-hump cnoidal waves, which behave as coupled solitary waves [79].

As known, the Bloch-Maxwell equation set for the SIT [72] has not only the solitary wave as a solution, but also an infinite periodic train. This solution describes cnoidal waves, which is especially inherent to waves with amplitude and phase modulation [72,80]. The electric field strength of cnoidal waves does not vanish anywhere, and their period is determined by the period of the Jacobi elliptic function, which is expressed in terms of the complete elliptic integral of the first kind. As its amplitude does not vanish, there is a nonzero polarization in a medium where this kind of wave propagates. This period becomes infinite and the cnoidal wave transforms into a solitary wave in the form of hyperbolic secant when the argument of complete elliptic integral becomes unity. The above-mentioned periodic solutions appear to be expressed in terms of elliptic functions as well; however, these our findings are only suggestive.

The question is whether it is possible to reduce the found periodic solutions to two solitary waves which may behave like a simulton copropagating, free of distortions, in the medium. To answer this question, we approximated one period of the found solutions by hyperbolic functions. The two-hump pulse may be approximated by a sum of two hyperbolic secant pulses with the same width and a sufficiently large time delay between them. The shape of A_1 may also be presented as a hyperbolic secant. Taking the ansatz

$$A_1 = \frac{2a_1}{\tau_1}\,\mathrm{sech}\left(\frac{\tau}{\tau_1}\right), \tag{60}$$

$$A_2 = \frac{2a_2}{\tau_2}\left[\mathrm{sech}\left(\frac{\tau-\mu}{\tau_2}\right) + \mathrm{sech}\left(\frac{\tau+\mu}{\tau_2}\right)\right], \tag{61}$$

and making use of the conservation laws (33)–(35), we can reduce the Eq. set (43)–(52) to equations for the parameters of the trial functions A_1 and A_2: a_1,a_2,τ_1,τ_2, μ. Here a_1 and a_2 are the amplitudes of the first and second pulses, τ_1 and τ_2 are their durations, and μ is a time delay between the pulses constituting the two-hump one. To fit the one- and two-humped pulses in widths, we assume that $\tau_1 = m\tau_2$ and $\mu = (m-1)\tau_2$, where m is an integer: $m = 2, 3, 4$. As earlier, for the sake of simplicity, we suppose that $\rho_{11} = \text{const}$. Then, for $\tau = 0$, we

arrive at the following set of algebraic equations:

$$4a_2^2m^2\mathrm{sech}^2\,(m-1)=\lambda^2a_1^2, \tag{62}$$

$$\varkappa\left\{a_1^2-\frac{4a_2^2m^4}{\lambda^2}\mathrm{sech}^4\,(m-1)\,[1-\sinh\,(m-1)]\right\}$$
$$=16a_2^2n_0'\tau_2^2m^4\mathrm{sech}^2\,(m-1)\,, \tag{63}$$

$$4a_2^2m^2\mathrm{sech}^2(m-1)\left[4\varkappa a_1^2-\left(\rho_{11}-\rho_{22}^0\right)m^2\tau_2^2\right]$$
$$=a_1^2\left[\left(\rho_{00}^0-\rho_{11}\right)m^2\tau_2^2-4\varkappa a_1^2\right]+2\varkappa a_1^2. \tag{64}$$

This set of equations is solved for the unknown variables a_1, a_2, and τ_2, depending on the parameters m and κ. Note that, to find the possible pulsed pairs, according to [5], for sufficiently long THz pulses the parameter $\kappa = 0.5\alpha_r c\tau_p$, where α_r is a resonant absorption coefficient and τ_p is the pulse duration. In the THz spectral range the resonant absorption coefficient of the ammonia vapor varies with respect to the pressure from 0.1 cm^{-1} at 200 hPa up to 5 cm^{-1} for 104 hPa. Consequently, for picosecond THz pulses, the parameter κ changes with increasing pressure from 0.035 to 0.7. In the next step we substitute the obtained solutions for A_1 and A_2 at $\tau = 0$ into the Maxwell-Bloch equations as the initial and boundary conditions and check their stability under the propagation in the molecular gas. Figure 4 shows the most stable couple of single- and double-hump pulses. In general, the pulse shapes are consistent with those found by numerical integration and shown in Fig. 3. The ratio of the wave amplitudes in Fig. 4 and Fig. 3 are in reasonable agreement in the central parts, but their behavior in the wings is slightly different. The asymptotic behavior of the two-hump pulse in Fig. 4 is not consistent with the conservation law (37). Therefore, the pair is not stable when it propagates. While a weaker pulse is more stable during propagation, the envelope of the two-humped pulse rapidly suffers from distortions. Figure 5 shows the latter at several distances in the vapor: at $z = 0, 1, 2, 3$ cm.

Perturbations of the two-humped pulse envelope become clearly visible for $z = 3$ cm, whereas for the first pulse they appear at much longer distances. Nevertheless, the bound state of this pulse pair is retained certainly. The mere fact that a two-humped pulse is robust to breakup originates from its interaction with the weaker beam. Figure 6 demonstrates an unstable scenario of nonlinear evolution of almost uncoupled

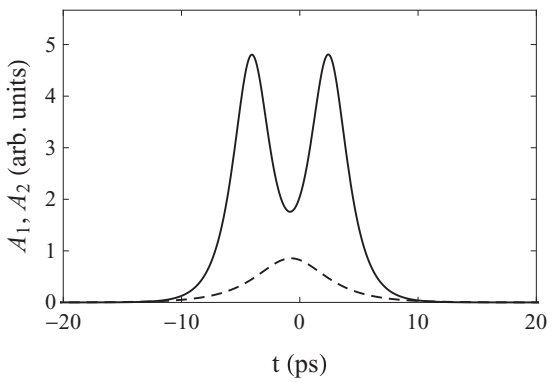

FIG. 4. Pulse pair as a result of an analytical approximation of the periodic solutions: A_2 (solid curve) and A_1 (dashed curve).

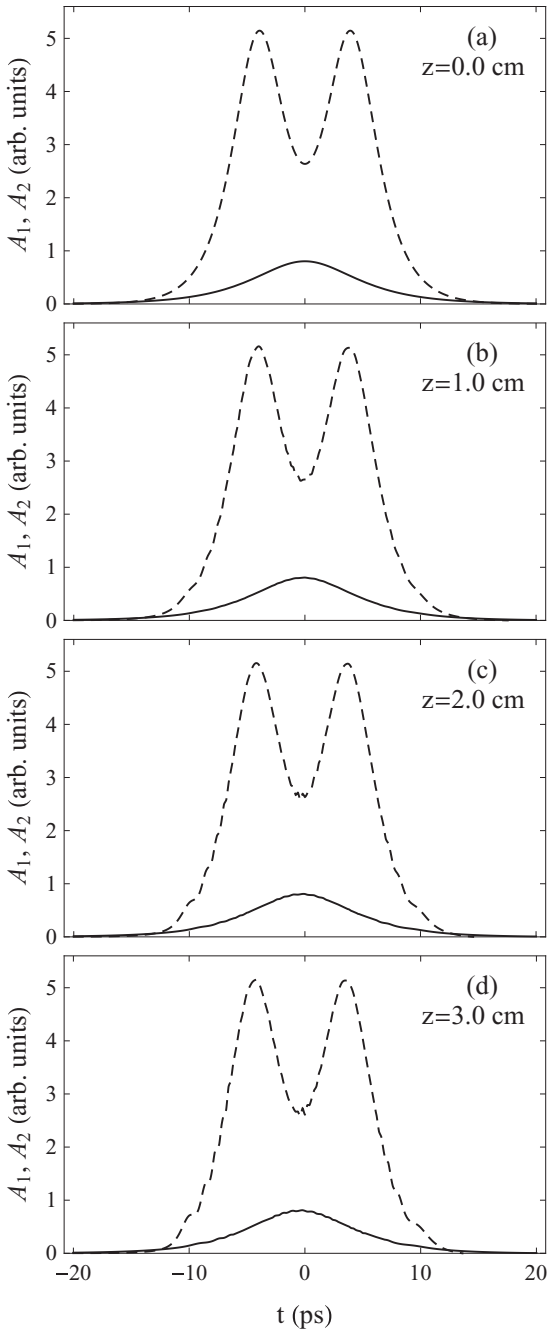

FIG. 5. Field propagation through the sample for pulse areas $\theta_1 = 1.61\pi$ and $\theta_2 = 9.92\pi$ (A_2 corresponds to the dashed curve and A_1 to the solid one).

pulses. Further analysis shows that a pair of three-humped and one-humped pulses is even more unstable under propagation. Interestingly, even a small dissipation makes the powerful pulse a little more stable to perturbations.

Numerical approximation of periodic pulse trains via hyperbolic secants allows us to get more stable solutions. So, Fig. 7 demonstrates a more stable propagation scenario for pulses with areas equal to 4π and 0.4π, respectively. At this, the powerful two-hump pulse is close to the sum of two hyperbolic secant pulses but differs a little. Both these pulses of equal width copropagate in ammonia vapors with the same group velocity in steady state for large-enough distances. One

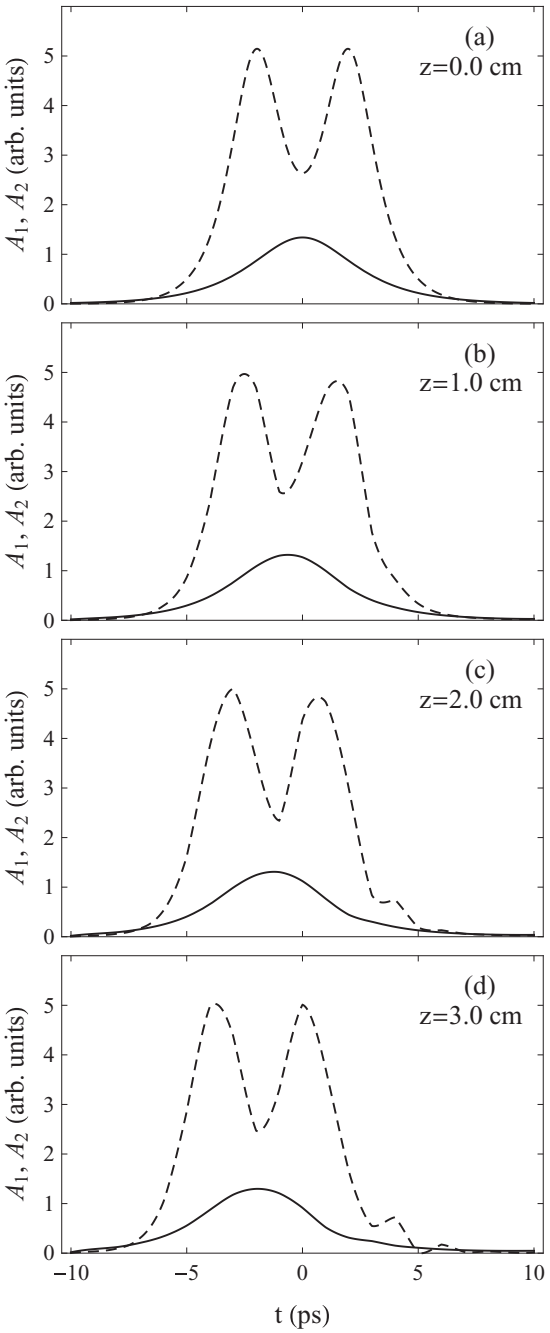

FIG. 6. Pulse pair propagation scenario for pulses A_2 (dashed curve) and A_1 (solid curve), with areas of $\theta_1 = 2.65\pi$ and $\theta_2 = 9.9\pi$.

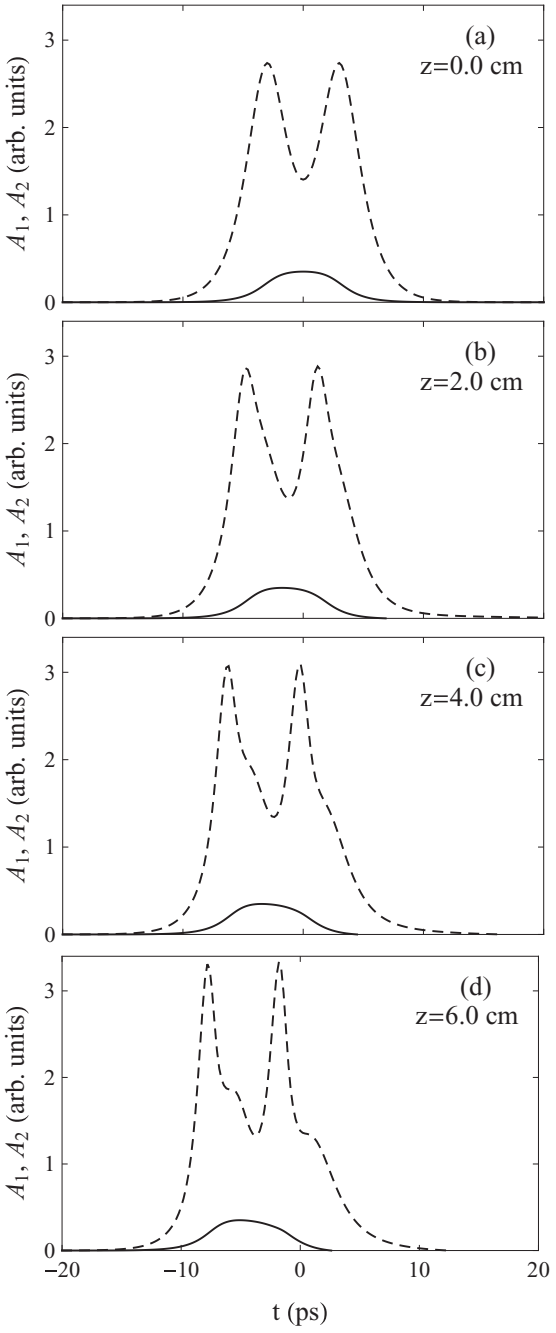

FIG. 7. Nonlinear evolution of the pulse pair: $A_1(t)$ (solid curve) and $A_2(t)$ (dashed curve), with $\theta_1 = 0.4\pi$ and $\theta_2 = 4\pi$.

can see that the two-humped pulse distortions begin when $z = 4$ cm, while the weak pulse retains its shape even at larger distances.

All of this speaks in favor of the formation of, at least, a quasisimulton. Moreover, the larger the dip of the two-hump pulse, the weaker is the pulse A_1. In this propagation regime, the weak pulse is stable and is sustained by the more powerful pulse, thanks to the energy exchange between both pulses and the medium. More precisely, the leading edge of the weak pulse A_1 is absorbed by the transition $0 \leftrightarrow 1$, while the first hump of A_2 first inverts the transition $1 \leftrightarrow 2$ together with all two-level systems and then induces a re-emission at frequency ω_2 by stimulated emission. The latter leads to an inversion of the $0 \leftrightarrow 1$ transition and induces the emission of a radiation at frequency ω_1, although the first pulse area is too weak to invert the $0 \leftrightarrow 1$ transition. These absorption and re-emission stages at frequency ω_2 are revived by the action of the second hump of the powerful pulse. After excitation, the molecules return to the ground state according to a Boltzmann distribution of the level populations.

Surprisingly, our results differ from data obtained in works [51,57] for the propagation of two optical pulses in a three-level medium with cascade transitions under stationary excitation of the upper transition. As mentioned above, at low excitation level the first pulse resonant with the lower

transition is two-humped and consists of two subpulses with areas approximately equal to 2π, whereas the second pulse is one humped. In our case, the situation is reversed. Indeed, the first pulse is weak and one humped, while the second one is much more powerful and two humped. We believe that the features of THz quasisimulton are due to the following factors: (i) rotational level configuration in ammonia, (ii) large-enough value of the oscillator strength of the upper transition in relation to the lower one ($\lambda = 2$). In Ref. [51], a two-humped solution has been obtained for $\lambda \ll 2$. Furthermore, all resonant levels in our case are populated initially. The stability of a pulse pair in ammonia is ensured by the fact that, although the powerful pulse does not make the medium transparent for the weak pulse by equalizing the populations of the resonance levels, it manages the energy exchange between the pulse A_1 and the medium at frequency ω_1 and hinders its dissipation. In other words, the powerful pulse adjusts the stage of absorption and emission of the weak wave. In this sense, we can say that the second pulse makes the medium transparent for the first one. In turn, the latter prevents the breakup of the former into separate pulses.

Figure 8 presents the scenario of the copropagation of two pulses that do not behave like a simulton. One can see that the pulse pair with the areas $\theta_1 = 1.6\pi$ and $\theta_2 = 4\pi$ is less stable during propagation in comparison to the quasisimulton presented in Fig. 7. Their group velocities are also inconsistent and the pulses separate gradually from each other.

Now, we consider the case corresponding to the first THz pulse too weak to affect the lowest transition noticeably. Then the second pulse may be one humped with an area of the order of 2π. Moreover, such a pair can be much steadier along the propagation axis (see Fig. 9) than the above-described pulse pairs. Specifically, two pulses with the areas $\theta_2 = 1.6\pi$ and $\theta_1 = 0.14\pi$ can propagate over very large distances, being little distorted. The weak pulse is free of distortion at distances up to 7.5 cm, while there are noticeable alterations for the more powerful pulse at this distance, as its area approaches 2π. Since the group velocities of the two pulses coincide, they travel together. However, the reason for the stability of this pulse pair is a little bit different. Here the second pulse forms a waveguide for the first one which is too weak to affect the population of the medium levels. A comprehensive analysis reveals other coupled states of two THz pulses under the conditions like an adiabatic population transfer in a three-level system, viz. $\rho_{11} = \text{const}$.

Differentiating Eq. (52) with respect to τ and substituting Eqs. (44) and (49), we obtain

$$\frac{\varkappa}{\lambda^2} A_2 \dot{A}_2 + \varkappa A_1 \ddot{A}_1 = A_1^2\left(\rho_{00}^0 - \rho_{11} - \varkappa A_1^2\right) + A_2^2\left(\rho_{11} - \rho_{22}^0 + 2n_0'\right) + 2n_0' A_2^2 \cos\theta_2, \tag{65}$$

in which we also employ expressions (31) and (32) and the solution of the equations governing the two-level subsystems. Collecting the terms with A_2 on the left side of this equation and the terms with A_1 on the right side and then dividing the resulting expression by the product $A_1 A_2$, it is easy to obtain

$$\frac{F(A_1)}{A_2} = -\frac{G(A_2)}{A_1} = C, \tag{66}$$

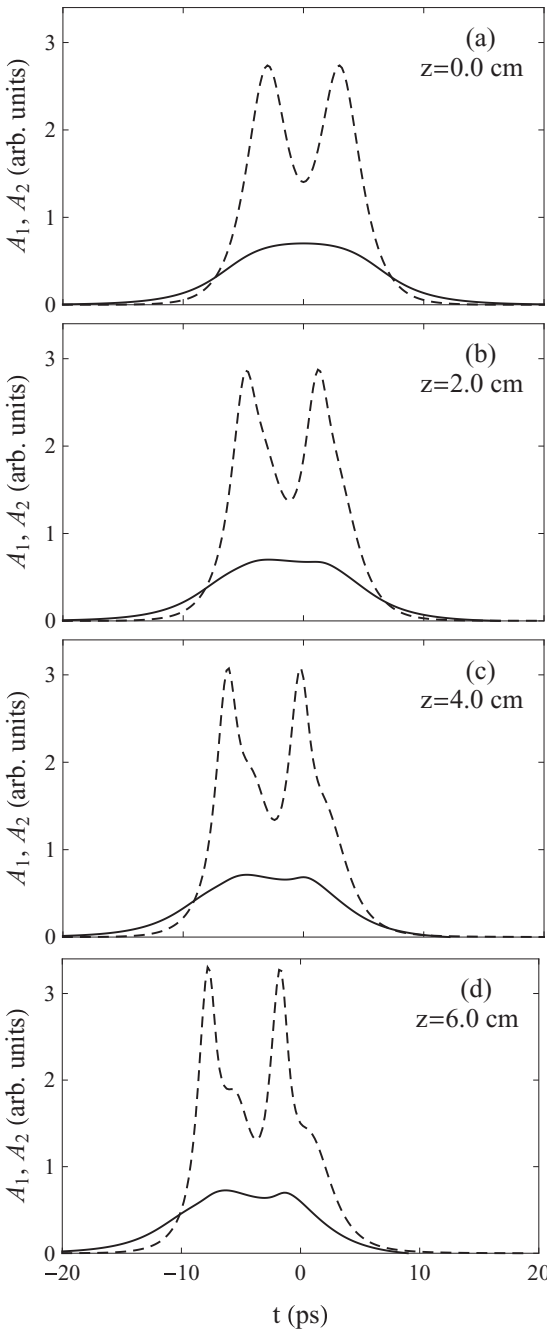

FIG. 8. Propagation dynamics of pulses that do not behave like a quasisimulton: $A_1(t)$ (solid curve) and $A_2(t)$ (dashed curve), with $\theta_1 = 1.6\pi$ and $\theta_2 = 4\pi$.

where $C = \text{const}$, $F(A_1) = \varkappa \ddot{A}_1 - A_1(\rho_{00}^0 - \rho_{11}) + \varkappa A_1^3$, and

$$G(A_2) = \frac{\varkappa}{\lambda^2}\ddot{A}_2 - A_2\left(\rho_{11} - \rho_{22}^0 + 2n_0'\right) + \frac{\varkappa}{\lambda^2} A_2^3 - 2n_0' A_2 \cos\theta_2.$$

Depending on C, a whole class of solutions for the fields can be deduced. However, the only valid solutions for fields will be those obeying the conservation law (37). Let us consider the possible solutions corresponding to $C = 0$. As a result, we

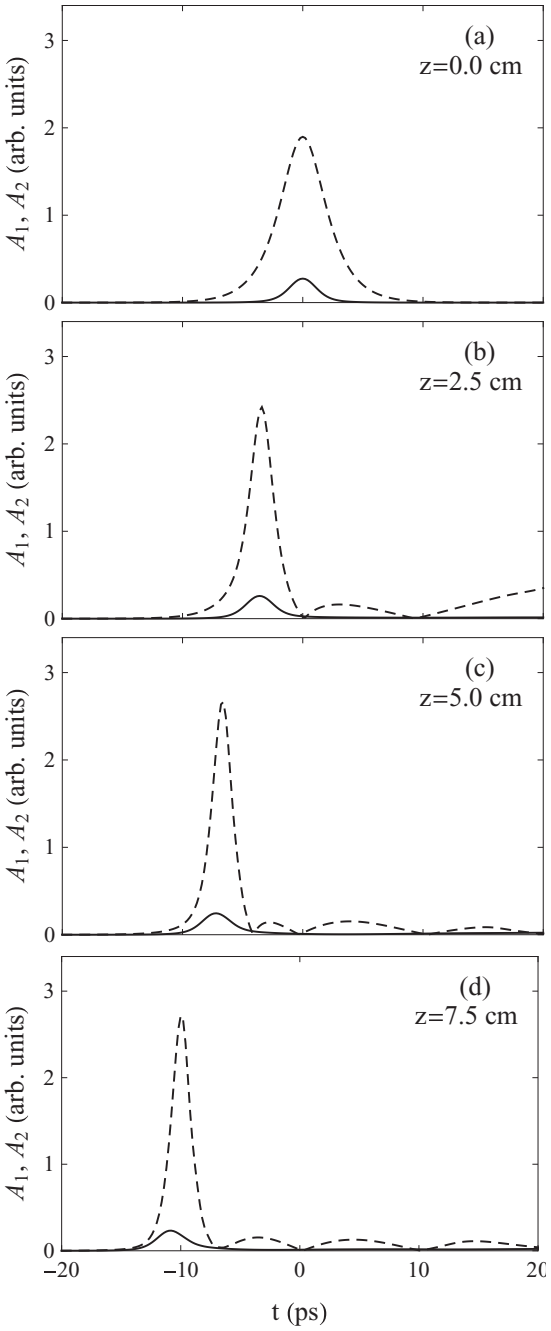

FIG. 9. Propagation of the pair consisting in two one-humped pulses: $A_1(t)$ (solid curve) and $A_2(t)$ (dashed curve), with $\theta_1 = 0.14\pi$ and $\theta_2 = 1.6\pi$.

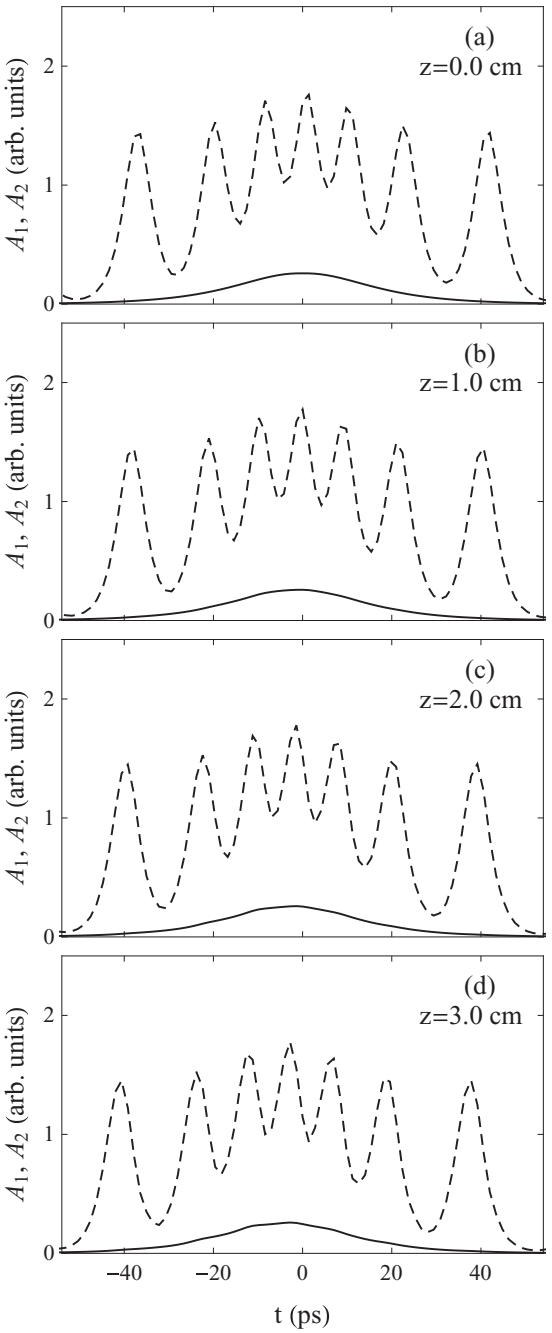

FIG. 10. Nonlinear evolution of the quasisimulton consisting of seven-humped and one-humped pulses: $A_1(t)$ (solid curve) and $A_2(t)$ (dashed curve); $\theta_1 = 1.7\pi$ and $\theta_2 = 14\pi$.

get the following equation set:

$$\frac{\varkappa}{\lambda^2}\ddot{A}_2 - A_2\left(\rho_{11} - \rho_{22}^0 + 2n_0'\right) + \frac{\varkappa}{\lambda^2}A_2^3 - 2n_0' A_2 \cos\theta_2 = 0, \tag{67}$$

$$\varkappa\ddot{A}_1 - A_1\left(\rho_{00}^0 - \rho_{11}\right) + \varkappa A_1^3 = 0. \tag{68}$$

As follows from Eq. (68), the solitary wave solution for the first pulse is a hyperbolic secant with a 2π pulse area. Equation (67) corresponds to a generalized nonlinear Klein-Gordon equation, whose analytical solution is problematic. However, the second pulse profile may be estimated by using the expression (37) which, for the sake of clarity, can be written as

$$A_2^2 = \lambda^2 A_1^2 + \frac{2n_0'\lambda^2}{\varkappa}\left(1 - \cos\theta_2\right). \tag{69}$$

It is evident that the second pulse area must be a multiple of 2π. At $\tau \to \pm\infty$ the amplitudes $A_1 \to 0$ and $A_2 \to 0$ obey the relation $A_2 \sim 2A_1$. According to our estimations, a multihumped pulse meets these requirements. We show in Fig. 10 a seven-humped pulse A_1 with an area of 14π and the corresponding single-humped pulse A_1 of hyperbolic secant shape. Surely, these pulses form a coupled pair. They have the

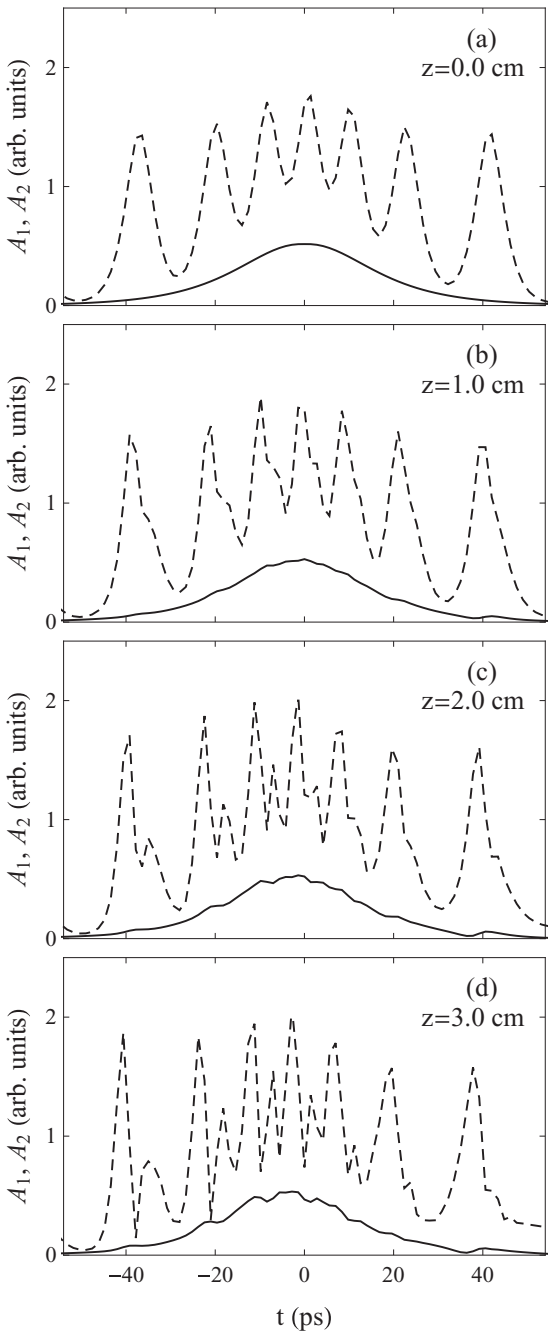

FIG. 11. Evolution of $A_1(t)$ (solid curve) and $A_2(t)$ (dashed curve) for the pulse pair not trapped by quasisimulton $\theta_1 = 3.4\pi$ and $\theta_2 = 14\pi$.

same width and propagate with equal group velocities over long-enough distances. At finite distances, these THz pulses are quite stable against distortions which allows us to think of this pulse pair as a quasisimulton.

The powerful pulse may contain not only odd, but also an even number of humps, depending on the first pulse intensity. While the solution has been obtained within the approximation $\rho_{11} = \text{const}$, the numerical integration of Eq. set (11)–(20) demonstrates a stable copropagation of these two pulses in a general case. Figure 10 proves the stability of the quasisimulton consisting of a seven-humped pulse with an initial area of 14π and a single-humped pulse with an area of 1.7π up to a distance of 3 cm. At larger distances, the more powerful pulse begins to distort a little bit, while the weaker one remains stable. Both pulses keep the same group velocities at distances up to 10 cm. When input pulse pair does not satisfy simulton solution, such pair is unstable under propagation. Figure 11 shows the evolution of THz pulses in molecular vapor not trapped by a quasisimulton. The distortions of powerful pulse are visible even at the distance of 1 cm. The first pulse is a little bit more stable.

The number of humps in the powerful pulse depends on the initial intensity of the weak pulse. The less intense the weak pulse, the more humped is the powerful pulse.

Let us now analyze how the first pulse impacts on the solution for A_2. Substituting into Eq. (65) the field A_1 expressed in terms of A_2 by means of (37), and simplifying a cumbersome expression by keeping only the terms linear in the small parameter n_0', we get

$$\frac{2\varkappa}{\lambda^2}\ddot{A}_2 + 2n'\frac{\dot{A}_2}{A_2}\sin\theta_2 - A_2\left[\frac{\rho_{00}^0}{\lambda^2} + \rho_{11}\left(1 - \frac{1}{\lambda^2}\right) - \rho_{22}^0 + 4n_0'\right] + \frac{\varkappa}{\lambda^2}\left(1 + \frac{1}{\lambda^2}\right)A_2^3 - 4n_0'A_2\cos\theta_2 = 0. \quad (70)$$

Taking the ansatz

$$\theta_2 = 4\arctan(e^{\nu t - \delta}) + 4\arctan(e^{\nu t + \delta}) \quad (71)$$

traditionally used for solving the double-sine-Gordon equation, we get

$$A_2 = \nu\left\{\operatorname{sech}(\nu t - \delta) + \operatorname{sech}(\nu t + \delta)\right\}. \quad (72)$$

After substitution of A_2 and its derivatives into Eq. (70), we obtain an algebraic equation for the parameters ν, δ, and $\varkappa$, which can be estimated numerically making use of the minimization methods varying the parameters over reasonable ranges. A typical solution consisting of two double-hump pulses with areas $\theta_1 = 2\pi$ and $\theta_2 = 4\pi$ for $\delta = 3.82$, $\nu = 1.04$, $\kappa = 0.36$ is presented in Fig. 12. Obviously, the second pulse, with an envelope presented in Figs. 3(a) and 3(b), is close to the 4π kink with an area of 4π [81]. However, in

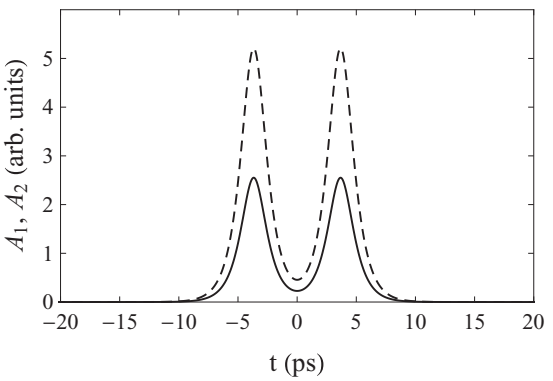

FIG. 12. Double-humped pulse pair as a solution of Eq. (70), $A_1(t)$ (lower curve) and $A_2(t)$ (upper curve): $\theta_1 = 2\pi$, $\theta_2 = 4\pi$, $\delta = 3.82$, $\nu = 1.04$, $\kappa = 0.36$.

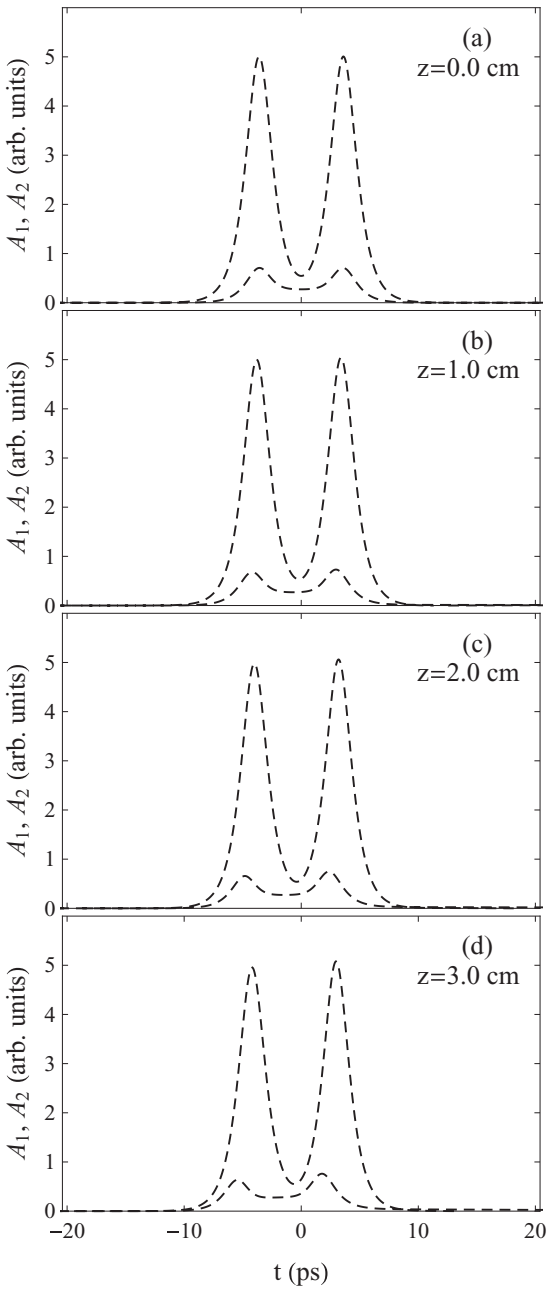

FIG. 13. Scenario of the behavior of the fields $A_1(t)$ (lower curve) and $A_2(t)$ (upper curve) for $\theta_1 = 2/3\pi$ and $\theta_2 = 4\pi$, whereas $\delta = 1.0$, $\nu = 3.60, \kappa = 0.017$ at the distances (a) $z = 0$, (b) $z = 1$ cm, (c) $z = 2$ cm, (d) $z = 3$ cm.

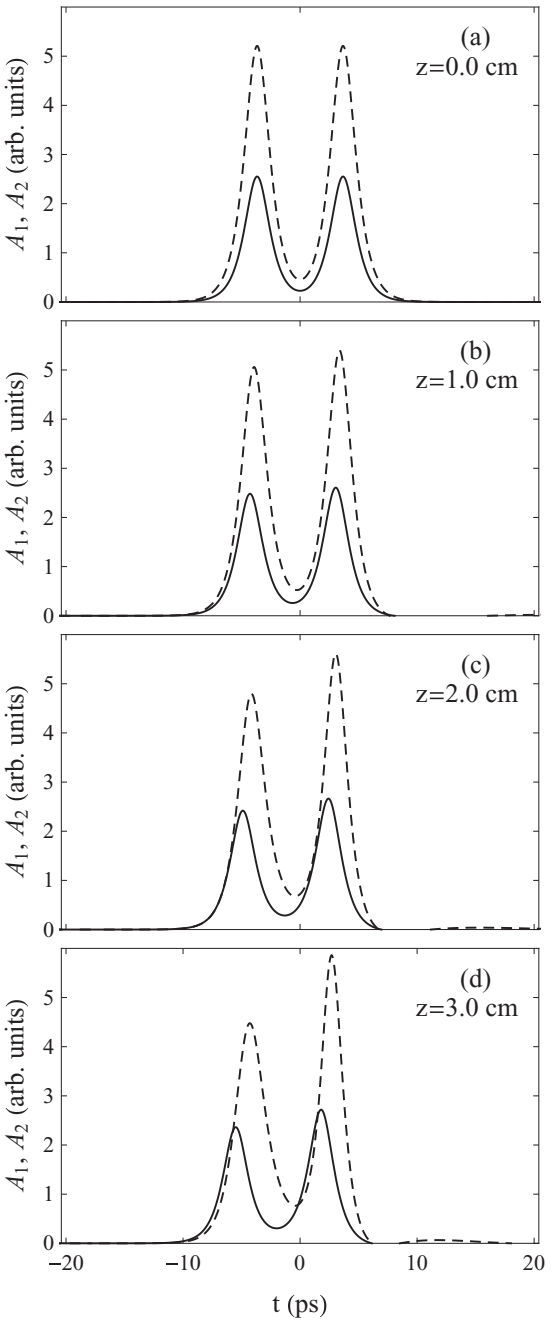

FIG. 14. Nonlinear evolution of the solutions (A_1 corresponds to the solid curve and A_2 to the dashed curve) presented in Fig. 12 for pulse areas $\theta_1 = 2\pi$, $\theta_2 = 4\pi$; the propagation lengths are (a) $z = 0$, (b) $z = 1$ cm, (c) $z = 2$ cm, (d) $z = 3$ cm.

contrast to the solution of double sine-Gordon equation, the value of dip δ in its profile is substantially larger.

The envelope of the first pulse has been obtained by use of conservation law (69). One can see that the weaker pulse as a whole replicates the shape of $A_2(\tau)$, which is also two humped. In other words, the last method gives us for $A_1(\tau)$ solutions significantly different from others obtained earlier. It is worth noting that the pairs consisting of two double-humped pulses are less stable compared to other pairs. Furthermore, the lower the amplitude of $A_1(\tau)$, the more stable is the pair of such pulses and the larger is the distance it can pass. Figures 13(a)–13(d) demonstrate nonlinear evolution of the most stable pair with the input pulse areas $\theta_1 = 0.75\pi$ and $\theta_2 = 4\pi$. Whereas the stronger pulse is free of distortions at a distance of 3 cm, the weaker pulse is unstable even at 1 cm. Its humps become asymmetric and its distortion increases with distance. Besides, because of the inconsistency of group velocities the second pulse is moving faster than the first one.

Figures 14(a)–14(d) show the unstable behavior scenario of the pulse pair with the following input data $\theta_1 = 2\pi$ and $\theta_2 = 4\pi$. One can see that both pulses are unsteady in the medium. Pulse asymmetry, manifested even at the distance of

1 cm, enlarges along the propagation axis. The group velocities are even more mismatched than in the previous case.

According to our preliminary estimations, the breather solutions for the pair of THz copropagating pulses are also available. Numerical analysis shows that such pairs may be stable at larger distances up to 10 cm. The corresponding results will be published in a forthcoming article.

As for copropagation of two few-cycle pulses, this case can be analyzed under quasiresonant conditions using a vector model for a three-level subsystem. The results obtained will be presented elsewhere.

VII. CONCLUSION

In conclusion, in this work we have studied the bound state of two terahertz solitary pulses copropagating in ammonia vapors and being in resonance with the lowest rotational transitions. More precisely, the transitions considered were the following: $K = 0$, $J = 0 \leftrightarrow 1, - \leftrightarrow +$ with the transition frequency $\omega_{01} = 0.6$ THz; $K = 0$, $J = 1 \leftrightarrow 2$, $+ \leftrightarrow -$, and $K = \pm 1$, $J = 1 \leftrightarrow 2, + \leftrightarrow -$, and $- \leftrightarrow +$ with the transition frequency $\omega_{12} = 1.2$ THz.

One of the THz pulses is resonant with the lowest transition of three-level system and another is in resonance with both the upper transition of three-level system and the other four two-level systems. The pulse envelopes are supposed to be shaped satisfy the SVEA. Thus, the problem is reduced to investigating two shaped THz pulses that propagate in a medium with two different multiplets that consist of three- and two-level subsystems, respectively. The coherent regime of interaction of both pulses with a medium is under study assuming their durations are less than the phase and population relaxation times.

We focused our attention on the conditions of trapping two THz pulses by simulton. Importantly, this problem is nonintegrable and it is significantly different from the task of propagating two light pulses in a three-level system with the cascade configuration of the levels [31,51,57]. On one hand, all relevant levels lying in the terahertz spectral range are populated at room temperature, which removes the conditions of population level pretreatment necessary to involve the upper transition in an interaction process in the optical region [31,51]. On the other hand, the presence of two-level subsystems certainly influences the scenario of trapping THz pulses by simulton. Besides, the fact that the oscillator strength of the lower transition is twice smaller than the others certainly complicates the trapping problem.

Using the Bloch equations for two- and three-level subsystems together with Maxwell equations, the conservation laws have been deduced. They describe the link between both fields and the medium and make easier the search for the coupled states of THz pulses. As follows from one of the conservation laws, the transitions between the lowest rotational states of the three-level multiplet are initiated by the weakest THz pulse. Another law binds the second pulse intensity with changes of the upper level population in the three-level system and with the population difference in the two-level systems. According to the third conservation law, the intermediate level is involved in a process of an energy exchange between two THz pulses and all multiplets in the ammonia vapor.

By use of conservation laws, the set of corresponding evolution equations for THz pulses has been obtained and an initial value problem (Cauchy problem) for obtained differential equations has been analyzed. The solutions in the form of solitary and periodic waves have been found. In the general case, the evolution equations are third-order differential equations which yield the periodic wave solutions.

It has been established that the powerful wave A_2 with a double-humped profile and the weak one-humped wave A_1 give rise to coupled state having the same periods and velocities. Moreover, in the absence of A_1, A_2 has a one-humped profile with a shorter period. Though the Bloch-Maxwell equations allow soliton-type pulse propagation for each THz pulse separately, searching for solitary wave solutions for two copropagating pulses is a very difficult task without an additional hypothesis on the behavior of the intermediate level population ρ_{11} or superposition state of upper and lowest levels ρ_{02}.

In order to find a pair of solitary waves satisfying the Maxwell-Bloch equations, the periodic solutions have been approximated analytically and numerically. For analytical approximation the trial functions have been taken in hyperbolic secant forms. The two-humped pulse assumed to be a superposition of two hyperbolic secants shifted to each other in time. In this case, the second pulse area is multiple to 4π. As for the weak pulse A_1, it is supposed to be hyperbolic secant. The widths of both pulses are supposed equal. Although such pulse pair certainly forms a coupled state, it is stable only at small distances. The pulse pair obtained via numerical approximation of periodic waves turns out to be a significantly more stable solution.

Two- and one-humped pulses have equal width and copropagate in ammonia vapor at the same group velocity. Moreover, the larger the dip value in the two-hump pulse is, the weaker may be the one-humped pulse. The two-humped pulse begins to distort at a substantially larger distance than 4 cm. At this, the weak pulse retains its shape even at larger distances. Their group velocities also keep the same magnitudes at distances up to 10 cm. All of this speaks in favor of, at least, a quasisimulton formation. The stability of the pulse pair in ammonia is originated from the control of absorption and emission of the weak wave in the medium by the powerful pulse. Thus, the second pulse makes the medium transparent for the first one. In its turn, the latter prevents the breakup of the former into separate pulses.

If the first THz pulse is too weak to affect the lower transition noticeably, then the second pulse may be one humped with the area close to 2π. Such a pair of two one-humped pulses is steadier in the medium than those mentioned above. When the first pulse is hyperbolic secant with area 2π, the second pulse may be multihumped with an odd or even number of humps. Such pulse pairs also demonstrate steady copropagation at finite distances and are quasisimultons in actual practice. Note that the evolution equations for THz pulses look like generalized nonlinear Klein-Gordon equations. Efforts were made to solve the evolution equation for the second pulse analytically, taking an ansatz used for solution of the double-sine-Gordon equation. In this case the second pulse is close to the 4π kink but with a large-enough dip. The weaker pulse replicates the shape of the more powerful pulse. However, such pairs of two double-humped pulses are shown to be unstable under propagation.

ACKNOWLEDGMENTS

We would like to thank E. Gaizauskas for fruitful discussions and V. Khassanov for help in preparation of the manuscript. We gratefully acknowledge the financial support from the European Commission (Mobility EMECW-Lot7-2232 and 602) and BRFFI (Grants No. F11F-009 and No. F12R-231).

[1] A. Demircan, Sh. Amiranashvili, C. Brée, Ch. Mahnke, F. Mitschke, and G. Steinmeyer, arXiv:1111.1989.

[2] R. K. Dodd, J. C. Eilbeck, J. D. Gibbon, and H. C. Morris, *Solitons and Nonlinear Wave Equations* (Academic Press, London, 1984).

[3] S. L. McCall and E. L. Hahn, Phys. Rev. **183**, 457 (1969).

[4] R. F. Slusher, Progr. Opt. **12**, 53 (1974).

[5] L. Allen and J. Eberly, *Optical Resonance and Two-level Atoms* (Wiley, New York, 1975).

[6] G. L. Lamb, Jr., Rev. Mod. Phys. **43**, 99 (1971).

[7] S. L. McCall and E. L. Hahn, Phys. Rev. Lett. **18**, 908 (1967).

[8] R. E. Slusher and H. M. Gibbs, Phys. Rev. A **5**, 1634 (1972).

[9] J. H. Eberly, Opt. Express. **2**, 173 (1998).

[10] C. K. N. Patel, Phys. Rev. A **1**, 979 (1970); J. J. Armstrong and O. L. Gaddy, IEEE J. Quantum Electron. **8**, 797 (1972).

[11] H. P. Grieneisen *et al.*, Appl. Phys. Lett. **21**, 559 (1972).

[12] J. J. Bannister, H. J. Baker, T. A. King, and W. G. McNaught, Phys. Rev. Lett. **44**, 1062 (1980).

[13] M. Jutte and W. von der Osten, J. Lumin. **83-84**, 77 (1999).

[14] O. Karni, A. Capua, G. Eisenstein, V. Sichkovskyi, V. Ivanov, and J. P. Reithmaier, Opt. Express **21**, 26786 (2013).

[15] G. L. Lamb Jr., *Elements of Soliton Theory* (Wiley, New York, 1980).

[16] A. A. Afanas'ev, R. A. Vlasov, and A. G. Cherstvyi, J. Exp. Theor. Phys. **90**, 428 (2000).

[17] A. A. Afanas'ev, R. A. Vlasov, O. K. Khasanov, T. V. Smirnova, and O. M. Fedotova, J. Opt. Soc. Am. B **19**, 911 (2002).

[18] A. I. Maimistov, A. M. Basharov, S. O. Elyutin, and Yu. M. Sklyarov, Phys. Rep. **191**, 1 (1990).

[19] K. Porsezian and K. Nakkeeran, Phys. Rev. Lett. **74**, 2941 (1995).

[20] K. Nakkeeran and K. Porsezian, J. Phys. A **28**, 3817 (1995).

[21] K. Nakkeeran, Phys. Lett. A **275**, 415 (2000).

[22] A. I. Maimistov, Quantum Electron. **40**, 756 (2010).

[23] O. K. Khasanov, D. V. Gorbach, S. V. Petrushkin, V. V. Samartsev, T. V. Smirnova, and O. M. Fedotova, Bull. Russ. Acad. Sci.: Phys. **70**, 621 (2006).

[24] P. J. Caudrey, J. C. Eilbeck, J. D. Gibbon, and R. K. J. Bullough, Phys. A **6**, L53 (1973).

[25] J. C. Eilbeck and R. K. J. Bullough, Phys. A **5**, 820 (1972).

[26] A. I. Maimistov, Quantum Electron. **30**, 287 (2000).

[27] S. A. Kozlov and S. V. Sazonov, J. Exp. Theor. Phys. **84**, 221 (1997).

[28] V. G. Bespalov, S. A. Kozlov, Y. A. Shpolyansky, and I. A. Walmsley, Phys. Rev. A **66**, 013811 (2002).

[29] E. V. Kazantseva, A. I. Maimistov, and J.-G. Caputo, Phys. Rev. E **71**, 056622 (2005).

[30] A. Yu. Parkhomenko and S. V. Sazonov, J. Exp. Theor. Phys. **87**, 864 (1998).

[31] M. J. Konopnicki and J. H. Eberly, Phys. Rev. A **24**, 2567 (1981).

[32] L. A. Bol'shov, T. K. Kirichenko, V. V. Likhanskii, M. I. Persiantsev, and L. K. Sokolova, Zh. Eksp. Teor. Fiz. **86**, 1240 (1984) [Sov. Phys. JETP **59**, 724 (1984)].

[33] J. H. Eberly, Quantum Semiclassical Opt. **7**, 373 (1995).

[34] Ya. I. Khanin and O. A. Kocharovskaya, Research Reports in Physics, Nonlinear Waves **3**, 162 (1990).

[35] M. O. Scully, S. Y. Zhu, and A. Gavrielides, Phys. Rev. Lett. **62**, 2813 (1989).

[36] M. O. Scully, Phys. Rev. Lett. **67**, 1855 (1991); J. H. Eberly, A. Rahman, and R. Grobe, *ibid.* **76**, 3687 (1996).

[37] S. E. Harris, Phys. Rev. Lett. **70**, 552 (1993).

[38] G. C. Dyer, G. R. Aizin, S. James Allen *et al.*, Nat. Photon. **7**, 925 (2013).

[39] R. Grobe, F. T. Hioe, and J. H. Eberly, Phys. Rev. Lett. **73**, 3183 (1994).

[40] M. J. Konopnicki, P. D. Drummond, and J. H. Eberly, Opt. Commun. **36**, 313 (1981).

[41] G. Assanto, C. Conti, and S. Trillo, J. Nonlinear Opt. Phys. Mater. **10**, 197 (2001).

[42] G. Leo, L. Colace, A. Amoroso, and A. Di Falco, Opt. Lett. **28**, 1031 (2003).

[43] S. O. Elyutin, A. I. Maimistov, and I. R. Gabitov, J. Exp. Theor. Phys. **111**, 157 (2010).

[44] A. Kujawski, Opt. Commun. **43**, 375 (1982).

[45] L. A. Bol'shov, V. V. Likhanskii, and M. I. Persiancev, Sov. Phys. JETP **57**, 524 (1983).

[46] A. I. Maĭmistov, Sov. J. Quantum Electron. **14**, 385 (1984).

[47] F. T. Hioe, Laser Physics **15**, 1355 (2005).

[48] P. D. Drummond, Opt. Commun. **49**, 219 (1984).

[49] S. Chelkowski and A. D. Bandrauk, J. Chem. Phys. **89**, 3618 (1988).

[50] H. Steudel, J. Mod. Opt. **35**, 693 (1988).

[51] L. A. Bol'shov and V. V. Likhanskiĭ, Sov. J. Quantum Electron. **15**, 889 (1985).

[52] A. Pusch, J. M. Hamm, and O. Hess, Phys. Rev. A **82**, 023805 (2010).

[53] A. I. Maimistov, Quantum Electron. **11**, 567 (1984).

[54] A. M. Basharov and A. I. Maimistov, Zh. Eksp. Teor. Fiz. **94**, 61 (1988) [Sov. Phys. JETP **67**, 2426 (1988)].

[55] A. Rahman and J. H. Eberly, Opt. Express **4**, 133 (1999).

[56] F. T. Hioe, Phys. Rev. A **26**, 1466 (1982).

[57] L. A. Bol'shov and A. P. Napartovich, Zh. Eksp. Teor. Fiz. **68**, 1763 (1975) [Sov. Phys. JETP **41**, 885 (1975)].

[58] M. Tonouchi, Nat. Photon. **1**, 97 (2007).

[59] D. Timothy, G. R. Baraniuk, and D. M. Mittleman, J. Opt. Soc. Am. A **18**, 1562 (2001).

[60] J. F. Federici, B. Schulkin, F. Huang, D. Gary, R. Barat, F. Oliveira, and D. Zimdars, Semicond. Sci. Technol. **20**, S266 (2005).

[61] B. M. Fischer, M. Walther, and P. Uhd Jepsen, Phys. Med. Biol. **47**, 3807 (2002).

[62] M. Nagel, P. Haring Bolivar, M. Brucherseifer, and H. Kurz, Appl. Phys. Lett. **80**, 154 (2002).

[63] K. Sakai, *Terahertz Optoelectronics*, 1st ed. (Springer, Berlin, 2005).

[64] R. Köhler, A. Tredicucci, F. Beltram, H. E. Beere, E. H. Linfield, A. G. Davies, and D. A. Ritchie, Opt. Lett. **28**, 810 (2003).
[65] H. Harde and D. R. Grischkowsky, J. Opt. Soc. Am. B **8**, 1642 (1991).
[66] H. Harde, J. Zhao, M. Wolff, R. A. Cheville, and D. R. Grischkowsky, J. Chem. Phys. A **105**, 6038 (2001).
[67] C. D. Amico, A. Houard, S. Akturk, Y. Liu, J. Le Bloas, M. Franco, B. Prade, A. Couairon, V. T. Tikhonchuk, and A. Mysyrowisz, New J. Phys. **10**, 013015 (2008); Y. S. You, T. I. Oh, and K. Y. Kim, Phys. Rev. Lett. **109**, 183902 (2012).
[68] L. Xu, X.-C. Zhang, and D. H. Auston, Appl. Phys. Lett. **61**, 1784 (1992).
[69] C. D'Amico, M. Tondusson, J. Degert, and E. Freysz, Optics Express **17**, 592 (2009).
[70] C. H. Townes and A. L. Schawlow, *Microwae Spectroscopy* (Dover, New York, 1975).
[71] J. M. Dowling, J. Mol. Spectrosc. **27**, 527 (1968).
[72] A. I. Maimistov and A. M. Basharov, *Nonlinear Optical Waves* (Kluwer Academic, Dordrecht, Boston, London, 1999).
[73] S. V. Sazonov and N. V. Ustinov, JETP Lett. **83**, 483 (2006).
[74] A. I. Maimistov, Pramana **57**, 953 (2001).
[75] J. R. Kuklinski, U. Gaubatz, F. T. Hioe, and K. Bergmann, Phys. Rev. A **40**, 6741 (1989).
[76] I. A. Poluektov, Yu. V. Popov, and V. S. Roitberg, Sov. Phys. Usp. **17**, 673 (1975).
[77] B.-F. Feng and T. Kawahara, Phys. D **137**, 237 (2000).
[78] B.-F. Feng and T. Kawahara, Phys. D **139**, 301 (2000).
[79] S. E. Haupt and J. P. Boyd, Phys. D **50**, 117 (1991).
[80] L. Matulic and J. H. Eberly, Phys. Rev. A **6**, 822 (1972).
[81] R. K. Bullough and P. J. Caudrey (eds.), *Solitons* (Springer-Verlag Berlin, Heidelberg, New York, 1980).